DETERMINATION OF WEAK TRANSMISSION LINKS BY CLUSTER ANALYSIS

A THESIS SUBMITTED TO
THE GRADUATE SCHOOL OF NATURAL AND APPLIED SCIENCES
OF
MIDDLE EAST TECHNICAL UNIVERSITY

BY

HAMZA OĞUZ ERTUĞRUL

IN PARTIAL FULFILLMENT OF THE REQUIREMENTS
FOR
THE DEGREE OF MASTER OF SCIENCE
IN
ELECTRICAL AND ELECTRONICS ENGINEERING

NOVEMBER 2009

Approval of the Thesis;

"DETERMINATION OF WEAK TRANSMISSION LINKS BY CLUSTER ANALYSIS"

submitted by **HAMZA OĞUZ ERTUĞRUL** in partial fulfillment of the requirements for the degree of **Master of Science in Electrical and Electronics Engineering Department, Middle East Technical University** by,

Prof. Dr. Canan Özgen _____
Dean, Graduate School of **Natural and Applied Sciences**

Prof. Dr. İsmet Erkmen _____
Head of Department, **Electrical and Electronics Engineering**

Prof. Dr. Nevzat Özay _____
Supervisor, **Electrical and Electronics Engineering Dept.**

Examining Committee Members:

Prof. Dr. Arif Ertaş _____
Electrical and Electronics Engineering Dept., METU

Prof. Dr. Nevzat Özay _____
Electrical and Electronics Engineering Dept., METU

Prof. Dr. Ahmet Rumeli _____
Electrical and Electronics Engineering Dept., METU

Prof. Dr. Nezih Güven _____
Electrical and Electronics Engineering Dept., METU

Abdullah Nadar (M.Sc.) _____
Manager, TÜBİTAK-UZAY

Date: 18/11/2009

I hereby declare that all information in this document has been obtained and presented in accordance with academic rules and ethical conduct. I also declare that, as required by these rules and conduct, I have fully cited and referenced all material and results that are not original to this work.

Name, Last name : Hamza Oğuz Ertuğrul

Signature :

ABSTRACT

DETERMINATION OF WEAK TRANSMISSION LINKS BY CLUSTER ANALYSIS

Ertuğrul, Hamza Oğuz
M.Sc., Department of Electrical and Electronics Engineering
Supervisor: Prof. Dr. Nevzat Özay

November 2009, 87 pages

Due to faults and switching, transmission lines encounter power oscillations referred as power swings. Although in most cases they do not lead to an eventual instability, severe changes in power flows on the lines may cause the operation of impedance relays incorrectly, leading to cascaded tripping of other lines. Out-of-Step tripping function is employed in modern distance relays to distinguish such an unstable swing but setting the parameters and deciding lines to be tripped require detailed dynamic power system modelling and analysis.

The proposed method aims to determine possible out-of-step (OOS) locations on a power system without performing detailed dynamic simulations. Method presented here, is based on grouping of the buses by statistical clustering analysis of the network impedance matrix. Inter-cluster lines are shown to be more vulnerable to give rise to OOS as proven with dynamic simulations on IEEE 39 bus test system.

Keywords: Power Swings, Out-of-Step, OST Relaying, Hierarchical Clustering

ÖZ

ZAYIF İLETİM HATTI BAĞLANTILARININ ÖBEKLEME ANALİZİ İLE BELİRLENMESİ

Ertuğrul, Hamza Oğuz
Yüksek Lisans, Elektrik ve Elektronik Mühendisliği Bölümü
Tez Danışmanı: Prof. Dr. Nevzat Özay

Kasım 2009, 87 sayfa

Arızalar veya anahtarlama operasyonları sebebiyle güç sistemleri güç salınımlarına maruz kalır. Bu salınımlar çoğu durumda nihai kararsız hal oluşumuna sebep olmasa da, iletim hatlarında mesafe koruma rölelerini yanıltan aşırı yük akışları oluşturarak diğer hatların da ardı ardına devre dışı kalmasına kadar giden sorunlar yaratabilmektedir. Günümüz mesafe koruma rölelerinde, açıklanan kararsız güç salınımlarını ayırt etmek amacıyla *out-of-step* işlevi mevcuttur. Ne var ki bu işlevin parametrelerini ayarlamak ve açılacak hatlara karar vermek güç sisteminin detaylı dinamik modellenmesi ve analizini gerektirmektedir.

Önerilen yöntem, güç sisteminde olası kararsız salınım noktalarının detaylı dinamik çalışmalar yapmadan belirlenebilmesini amaçlamaktadır. Sunulan yöntem, güç sistemi empedans matrisinin istatistiksel öbekleme yöntemi ile analiz edilmesi üzerine kuruludur. Öbekler arası hatların kararsız salınımlara daha açık olduğu IEEE 39 bara test sistemi üzerinde yapılan dinamik benzetim çalışmalarıyla ispatlanmıştır.

Anahtar Kelimeler: Güç Salınımları, OST Röleleme, Hiyerarşik Öbekleme

to my mother,

dear brother,

lovely wife

and

to the sincere memory of my father

ACKNOWLEDGMENTS

The author wishes to express his deepest gratitude and respects to his supervisor, Prof. Dr. Nevzat Özay for his guidance, advice, criticism, encouragements, insight and patience throughout the research.

The author would also like to thank Ms. Yıldız Durukan and Ms. Algı Özkaya from TEİAŞ, Europe Transmission Coordination Division for their sincere supports throughout the study.

Suggestions and comments of Mr. Melih Güneri as well as guidance and friendship of Mr. Müfit Altın are greatly appreciated.

Cooperation and friendship of Mr. Burçak Kurt added significant value to this study.

Finally, I would like to thank to my family for their support and guidance through all stages of my life.

TABLE OF CONTENTS

LIST OF TABLES

LIST OF FIGURES

CHAPTER 1

INTRODUCTION

Transmission systems are experiencing a transition from being operated as national grids to international networks following the political transition from nations to international political unions like European Union. ATCo, NORDEL and former UCTE (now ENTSO-E) are examples of system operators with large synchronous interconnected systems.

As transmission systems are expanded, both in terms of length and capacity, they will be more vulnerable to be threatened by operational impacts like switching and undesirable impacts like faults.

Just like other dynamic systems, change of a variable in the operating state of a power system, will disturb the steady state point and will cause impacts named as power swings.

Theory of power swings is very well explained in 1950s by German engineer; Rüdenberg [1]. Power swings and their impacts on transmission system are basically introduced in Chapter 2.

Transmissions systems are invariably protected by distance protection relays which measure the impedance of the line by taking the ratio of voltage to current. During a power swing, the impedance measured may indicate a faulty condition although the system will remain healthy. False tripping of the faultless line, normally, alleviate the stability condition, leading to cascaded

tripping of the other lines. Theory of the impedance relays is given in chapter 3.

The effects of power swings on the operation of distance relays are controlled by dynamics of the power system. However, as in the system like UCTE, with very high number of buses and generators, it is very difficult to simulate (and verify) the dynamic conditions due to impacts on power system.

Therefore; an alternative approach for the determination of weak transmission lines, on which power swings are most likely, is necessary. Once these lines are identified, dynamic simulations can be carried out with these lines in mind.

Impedance matrix of a network contains static network parameters not dependent on current operating point and branch loading levels. Chapter 4 is devoted to the well-known impedance matrix and its implicit properties.

Starting with the invention of digital computers, ways of storing and processing vast data are invented and applied in many branches of science and engineering. Vast data are processed by means of statistical methods in order to explain imponderable properties of multi-variable systems.

In this thesis work, Z matrix elements of the sample IEEE 39 bus system are analyzed and similarities obtained by data clustering techniques are used to identify the possible weak links of the power system. Out of step conditions are much likely to exist in these weak links if the theory presented here is correct.

Z matrix is necessarily computed within the algorithm while a load flow calculation is performed. Hence, obtaining the impedance matrix for real power systems will not serve additional burden to the analysis techniques. For online security assessments conducted by the operators real-time in the dispatching centers, this method will be appropriate to define the possible out of step conditions that may arise with changing loading levels. By means of a system planning approach, possible out-of-step locations can easily be estimated

leading to a pre-analysis of the network configuration without need of detailed dynamic simulation.

Data clustering method applied in this thesis is briefly explained and application of data clustering to IEEE-39 bus test system is performed in Chapter 5.

Simple algebraic formulations are valid for the calculation of static parameters whereas differential equations are employed for dynamic calculations which necessitate the use of challenging numerical iterations. Although there is no fully-static system preserving its operational point forever, static systems are more preferred in the analysis view to get rid of the computational burden of the transient behaviours in dynamic systems. Dynamic properties are tried to be predicted by the use of static data in this study.

However, it should be pointed out that, static approximations on the dynamical system parameters will be valid near to operating point behaviour. They would, necessarily, employ natural approximation errors as dynamic behaviour moves away from operating point. Validity of the static approximation of the thesis work should be verified by dynamic simulations.

The clustering theory, utilizing Z matrix, developed for the analysis of weak lines is tested on IEEE 39 bus test system. After determination of the lines, effects of power swings are tested with dynamic simulations in Chapter 6.

Application of the theory is performed for Turkish 380 kV system in Chapter 7. Possible weak links are identified for the Turkish system by applying clustering method.

CHAPTER 2

POWER SWINGS

2.1 SYNCHRONIZING FORCES IN ALTERNATING MACHINERY

> Synchronous machines for three-phase current will work in perfect parallel operation if their frequencies and voltages coincide and if their mechanical input or electrical output is appropriate to their sizes so that the angle between corresponding poles of the various machines remain within moderate limits [1].

Switching operations on the network may disturb the equilibrium and may cause machines to fall *out-of-synchronism.*

By assuming the terminal voltage V_T is given constant by connection to a very large system, electric phenomena in the machine is surveyed by the phasors diagram in *Figure 2.1*. Neglecting the small resistive component of the stator winding; leakage voltage E_s of the stator winding and the voltage E_q of the full quadrature armature reaction, both are perpendicular to the current I of the machine, are added up to form the resultant electromotive force E_i of the machine.

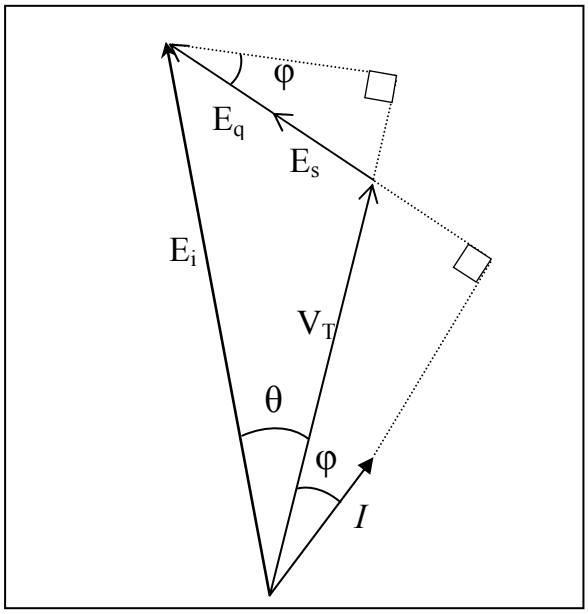

Figure 2.1: Voltage phasors of the machine

It can be seen that machine terminal voltage V_T and total emf *Ei* has a phase difference of θ which is referred as the machine pole angle. By using the general formulation of the real part of the complex power; active electrical power output of a synchronous machine is simply;

$$P = V_T . I . \cos\varphi \tag{2.1}$$

Where φ is the phase angle between terminal voltage *E* and current *I.*

By referring the upper triangle in *Figure 2.1*; we can deduce

$$(E_s + E_q)\cos\varphi = E_i \sin\theta \tag{2.2}$$

And substitute *cos(φ)* term in Eqn. (2.1),

$$P = V_T . I . \frac{E_i}{E_s + E_q} \sin\theta \tag{2.3}$$

$$P = P_{\max} \sin\theta \tag{2.4}$$

This formulation gives rise to the well known swing curve shown in *Figure 2.2*. With changing the machine pole angle θ, electric power output of the synchronous machine varies according to the sine curve in *Eqn 2.4*.

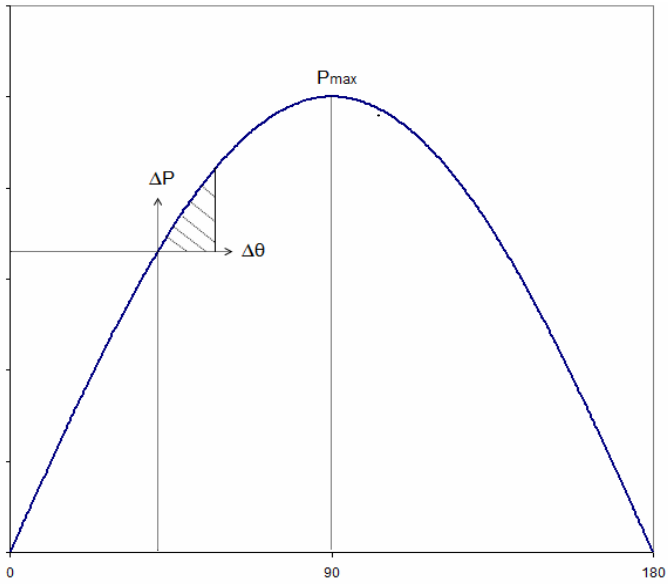

Figure 2.2: Swing Curve

The mechanical input, directly related to the admission of energy to the prime mover, however, is left constant. As a result, if mechanical energy is larger than the electrical output, generator accelerates, and it retards if electrical power is larger. The excess power in both situations, for small changes in angle θ can be approximated by;

$$\Delta P = \frac{dP}{d\theta} \times \Delta\theta = P_s \times \Delta\theta \qquad (2.5)$$

Where the factor P_s is named as the *synchronizing power*, trying to restore the pole wheel to the synchronous position.

The synchronizing power is found by the differentiation of *Eqn 2.4* as;

$$P_s = P_{\max} \cos\theta \qquad (2.6)$$

Be aware that $P_{\max}\cos\theta$ is not constant and depends on the value of θ. Hence each incremental pole angle adjustment ($\Delta\theta$) will not give rise to the same re-synchronization effort by the machine. Machine will try to reach to synchronization with an effort related to the initial pole angle value. Then, there exists points that are more probable to reach synchronization or to preserve synchronism in some part of the swing curve. Since it is a cosine function, these points corresponds to the very beginning of the angle axis i.e. small angle values. That is why angle difference is adjusted as 15^0 or 20^0 operationally for medium length lines.

Additionally; synchronizing effect of the P_s is true only for the rising branch of the power-angle curve. If the angle exceeds 90^o during acceleration, P_s becomes negative trying to pull the machine out of synchronism further.

Theory in here is presented for a single machine case. The transmission limit for the two machines or multi-machine case is similar in theory in the sense that available power transfer between two buses is dependent on the angular difference between the buses. Bus angle difference in the multi-machine case is similar to the pole angle in one machine case. Hence, power swing theory can be extended to multi-machine cases.

2.2 STABILITY UNDER POWER IMPACTS

If the electrical load (P) of a synchronous machine is increased by admission of energy to the prime mover (i.e. by increasing P_{mech}), at the same time and with small increments, the operating point may approach the top-level (90^o) of the swing curve in *Figure 2* without pulling the machine out-of-step.

If, however, same load increment is applied as a sudden power impact, the machine swings considerably far beyond the steady state value of the pole angle.

The power of inertia, P_J, is determined by the difference between the mechanical driving power and electrical output power. The power balance in the machine is;

$$P_J = P_{mech} - P \tag{2.7}$$

This difference is shown shaded in *Figure 2.3*. Free potential energy is then calculated by integration as;

$$W_J = \int (P_{mech} - P) d\theta \tag{2.8}$$

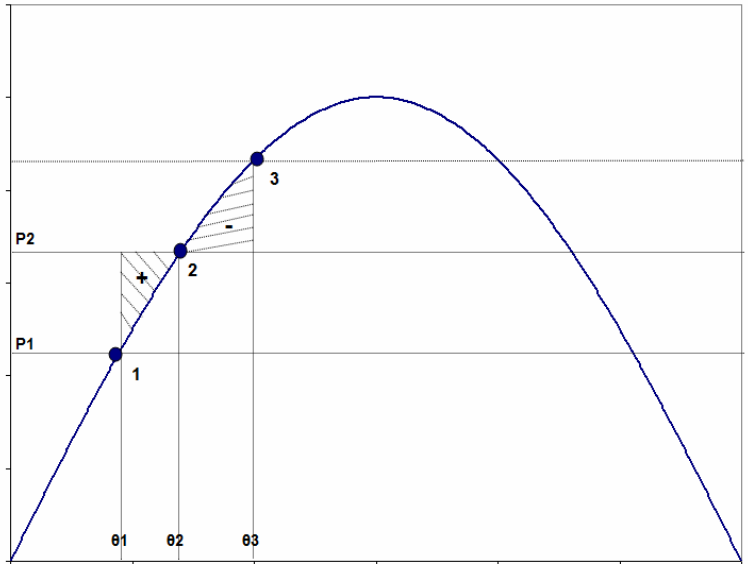

Figure 2.3: Equal-Area Criterion

Every impact of load causes the stationary point on the power angle curve travel from point 1 to point 2 on *Figure 2.3*. Energy set free on the pole wheel according to *Eqn 2.8* will cause an increase in machine speed up to a certain maximum point (i.e., point 2). By that means, the pole wheel overshoots to position of point 2 and retarded from now on since the area is negative and the motion is reversed on point 3. The angle of this reversal point is determined by the equality of areas causing acceleration and deceleration.

Excess angle of oscillation θ_3-θ_2 becomes larger than the initial angular

deviation θ_2-θ_1 of the power impact because of the curvature of the slip characteristics as considered in [1]. Inequality of θ_3-θ_2 and θ_2-θ_1 can also be explained with a graphical approach to the sine curve.

If the synchronous machine has a damper winding (or if there is a resistive component within the network supplied by the machine), the free potential energy of the shaded areas in *Figure 2.3* will gradually be absorbed and the preceding swings of the pole wheel will move closer to point 2 than the first swing in each swing period. The power of inertia given by *Eqn 2.7* is now reduced by the damping power P_σ which is dependent on the movement of pole wheel.

$$P_J = P_{mech} - P - P_\sigma \tag{2.9}$$

Hence, the initial overshoot of the power swing will be greater than the preceding ones in the real systems for which there are resistive damper components. That is why *"first swing stability"* is of the main concern in practical cases. In this thesis work, derivations in this chapter are performed by neglecting the resistive components for simplicity of the equations. However in simulations performed to verify the theory, resistive components are included in the network parameters.

If the synchronous machine is not connected to a rigid network but to another synchronous machine, the terminal voltage, V_T, in *Eqn 2.3* will not remain constant. *Eqn 2.3* should be modified to eliminate the variance of terminal voltage, V_T, so that;

$$\frac{E_s + E_q}{I} = X_S + X_q \tag{2.10}$$

The available synchronous power appears in the form;

$$P = \frac{V_T . E_i}{X_S + X_q} \sin \theta \qquad (2.11)$$

where θ still defines the angular difference between internal emf and terminal voltage.

Eqn 2.11 is true whether V_T remains constant or its magnitude and angle are changing.

Eqn 2.11 can be broadened to a two machine system by integrating the machine internal emf's, E_{i1} and Ei_2, and summing the reactances of the transmission line and the two machines together.

$$P = \frac{E_{i1} . E_{i2}}{X_T} \sin \theta_{12} \qquad (2.12)$$

Here θ_{12} refers to the phase angle between the internal emf's of the two separate machines and X_T term includes all the transmission line, transformer and machine leakage and quadrature axis reactances together.

Power impact, whether it is a load switching or a fault, will be distributed between the machines connected to the network. This will create a power oscillation within the transmission lines which is defined as a power swing. Swings are the oscillations of synchronous machines with respect to other synchronous machines.

A swing does not necessarily lead to system instability. Period and type of the power swing will determine the stability limit of the network and as a result stability may be disturbed leading to cascaded out-of-step (instability) conditions within the network.

Large power swings whether they are stable or not, may cause unwanted relay operations at different network locations [2]. Distance and other types of relays should not (intentionally or unintentionally) trip during dynamic system conditions. Power Swing Blocking function (PSB), which intends to block tripping of distance relays during swings, is available in modern distance relays.

CHAPTER 3

DISTANCE PROTECTION OF TRANSMISSION LINES

3.1. BASICS OF POWER SYSTEM RELAYING

In power systems, relays are used to detect abnormal operating conditions by monitoring basic power system variables such as voltage, current, power flows or system frequency. Entire subject of the protection is governed by the general requirements which can be listed as; correct diagnosis of trouble, quickness of response and minimum disturbance to the rest of the power system.

Relaying action ensures that the remaining system is still fed with power and protects the system from further damage due to the fault. Since quickness of relay response and isolating the fault region are vital to protect the system from further damage, relays are equipped for every step of the power system.

There are two groups of the relaying equipment, namely; primary relaying and the back-up relaying. Since selectivity is one of the main concerns to isolate the faulted region, power systems are subdivided into protective zones protected by unit protection schemes (i.e., primary relaying). Primary relaying is first line of defense whereas back-up relaying is adjusted to operate when primary line of defense fails to operate due to any reason. *Figure 3.1* shows the basic equipments of the primary relaying within every level of the power system.

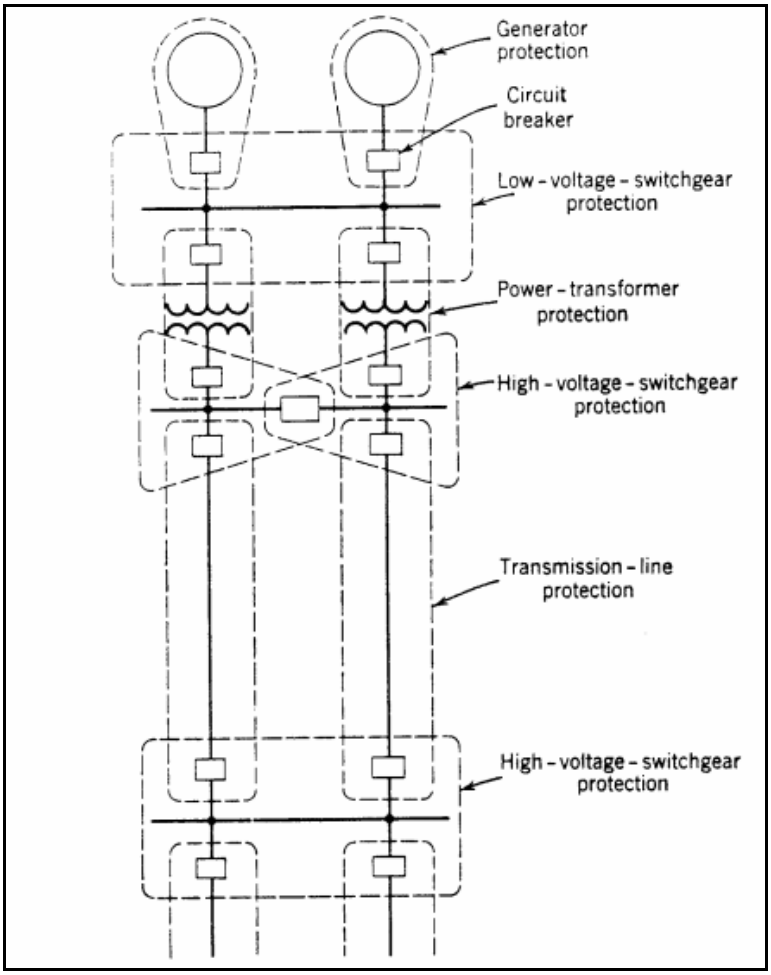

Figure 3.1: Portion of a power system illustrating primary relaying [3]

As can be traced from the figure, protective relaying components are equipped in every step, for all equipment within a power system. They should be well coordinated with each other in order to isolate the faulted or abnormally operating part of the system to avoid cascaded tripping.

This study is mainly focusing on the abnormal conditions occurring on transmission lines. Hence, relays used to detect abnormal conditions in transmission lines are of primary interest for this study.

The necessity for highly reliable, fully discriminative, high-speed protection is absolute in the context of 400 kV transmission systems [4]. Economic aspect of the protection can not be ignored; but that it comes second in order of

priority when dealing with the protection of transmission lines.

Transmission lines are protected by distance relays. Theory of distance protection is worth to be mentioned here.

3.2. DISTANCE PROTECTION

Distance protection is a non-unit protection whose operation and selectivity depend on local measurement of electrical quantities [5]. Local measurement would necessarily employ measurement errors. Therefore, it is not practically possible to exactly (i.e. 100%) protect the unit and to perform full selectivity with distance protection.

Zone grading is employed in distance relays with instantaneous zone of 85% to compensate the measurement errors. Because of its various zones, distance protection is not a full-unit protection. However, it is possible to perform an effective unit-protection by integrating communication channels between two distance relays on two ends of the line. This is achieved by power line carrier signals injected by capacitor voltage transformers at one end and then, picked by the same device at the other end. Line traps are employed to prevent signals dispersing to other lines in the network. Fiber optic cables are also used for communication purposes.

When carrier and signaling equipment is not available, conventional distance scheme is used with most remote 15-20% segment of the line is protected by the second zone not the first zone.

3.2.1 Basic Principle of Distance Protection

Distance relays are main devices for the protection of transmission lines especially for HV and EHV lines. A distance relay has the ability to detect a fault within a pre-set distance along a transmission line or a cable. Every power

line has its reactance and resistance values per kilometer defined by its design parameters which will make the total impedance of the power line a function of its total length. A distance relay employing a current and a voltage measuring unit, just looks for the current and voltage magnitudes and estimates these two on the basis of Ohm's law to calculate the Z (impedance) value.

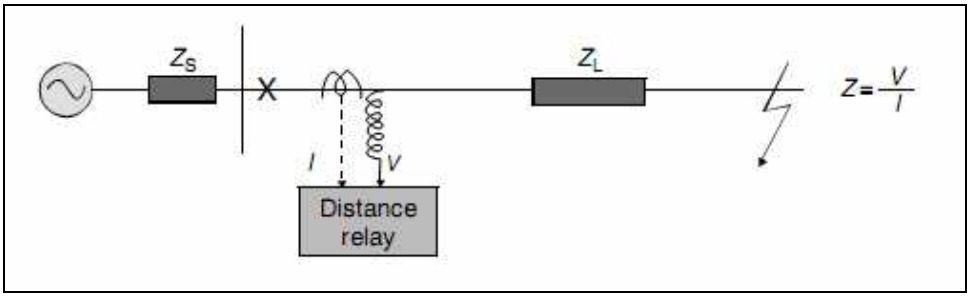

Figure 3.2: Basic distance protection principle

Operation principle of a distance relay is best visualized by a balanced beam relay configuration in *Figure 3.3.* Voltage data is fed onto one coil whereas current data is fed onto the other to provide a restraining torque to balance the beam on normal operating conditions. Under fault conditions, current increases dramatically whereas voltage collapses in extreme cases, unbalancing the beam and closing the contacts for the initiation of the tripping action. By changing the turn ratio of an ampere coil to voltage coil, the impedance reach of the relay can be adjusted.

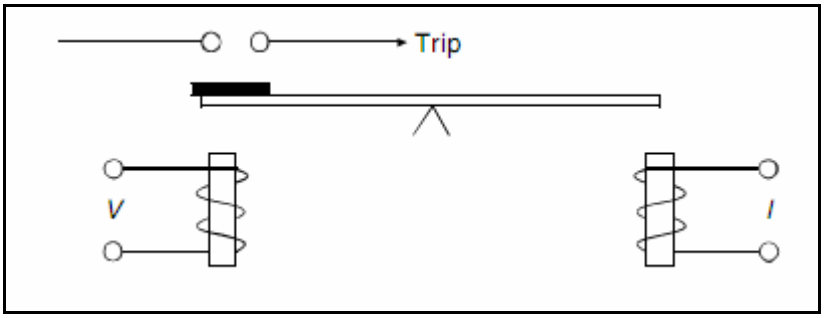

Figure 3.3: Balanced beam configuration

3.2.2 Tripping Characteristics

Tripping characteristics of a basic distance relay may be plotted on an R-X diagram as shown in *Figure 3.4.* It is a simple circle with its center at the origin named as plain impedance characteristics. Relay will operate for all the impedance values entering within the circle not taking into account the phase angle between voltage and current. (Non-directional characteristics)

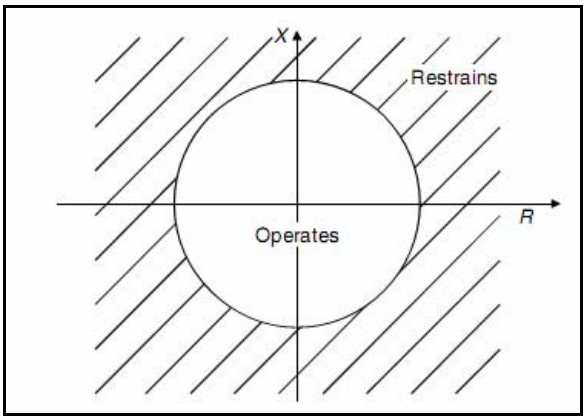

Figure 3.4: Plain impedance relay characteristic

A non-directional relay can be polarized by feeding additional voltages on additional voltage coils in *Figure 3.3* to compare the phase angles of voltage and current. This will move the circular region such that the circumference passes through the origin leading to the widely used MHO impedance relay characteristics in *Figure 3.5*. Angle θ is known as the relay's characteristic angle.

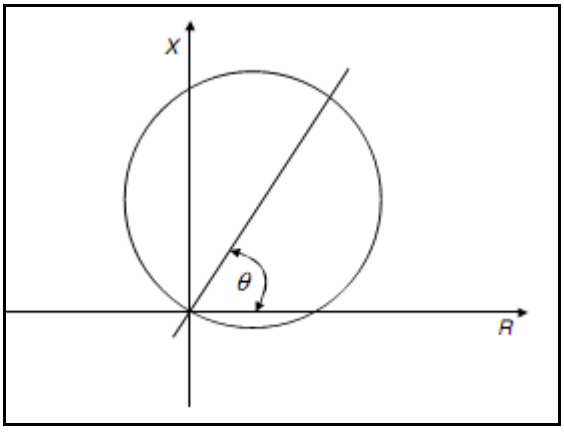

Figure 3.5: MHO characteristic

3.2.3 Zone and Time Grading in Distance Relays

Basically, measured impedance by a distance relay is compared with the known line impedance. If measured impedance is smaller than the line impedance, an internal fault on the line is detected and trip command is issued to the circuit breaker.

Due to inaccuracies in measurement, basically resulting from CT errors and inaccuracy of the line impedance, 100% protection zone is not possible in practice. A margin of 15-20% is chosen and the under-reach zone of the relay is generally used as 80-85% of the known line impedance. Under-reach zone is also defined as the 1^{st} zone and tripping is instantaneous in that zone.

Remainder of the line and some part of the next transmission line is protected by an over-reaching zone (2^{nd} zone). As over-reach zone is the back-up protection of the under-reach zone for the next line segment, it must be delayed to ensure selective protection. Time delay of 250-300 ms is used in modern numerical relays. Selective tripping is performed by time grading in distance relays.

Additional third zone is generally employed with greater time delay. 3^{rd} zone is adjusted for 120-180% of the line with time delay of 0.8 seconds. Some configurations use 3^{rd} zone as looking to reverse direction with greater time delay, namely for back-up protection to previous line segments.

Distance relays are equipped in both ends of the line aiming to isolate the fault on the line by opening circuit breakers at both ends instantaneously as seen in *Figure 3.6.*

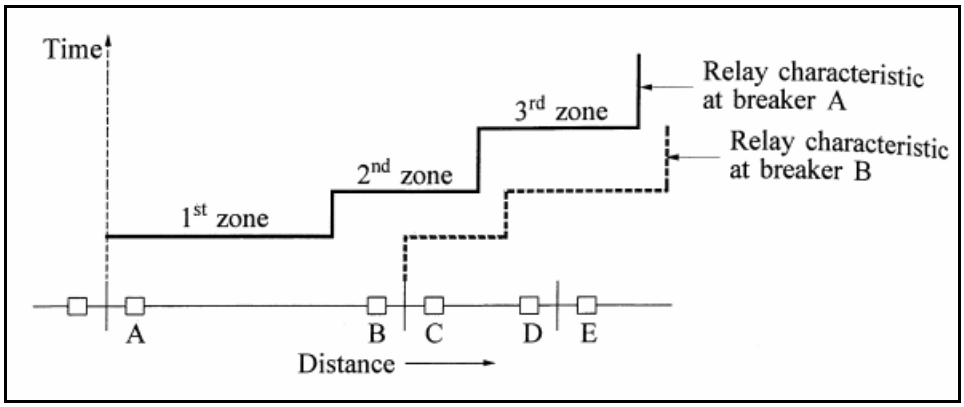

Figure 3.6: Protective zones and time grading

3.3 EFFECT OF POWER SWINGS ON LINE RELAYS

Distance relays respond to the impedance between the relay location and fault location. They simply process the data measured by voltage and current transformers and decide the tripping action when an abnormal condition is met.

Power swings can; for example, cause the load impedance, which under steady state conditions is not within the relays operating characteristics to enter into relays operating characteristics. Operations of these relays during a power swing may cause undesired tripping of transmission lines, weakening the system and thereby leading to cascaded outages [6]. Unintentional tripping of distance and other types of relays should be blocked by allowing power system return to a stable state.

3.3.1 Power Swing Blocking Function in Distance Relays

Power Swing Blocking (PSB) function is used in modern distance relays in order to differentiate between fault and a power swing. PSB is simply performed by placing checkpoints on pre-determined locations of the R-X plane. These checkpoints are named as “blinders”. A simple two-blinder scheme is shown in *Figure 3.7.*

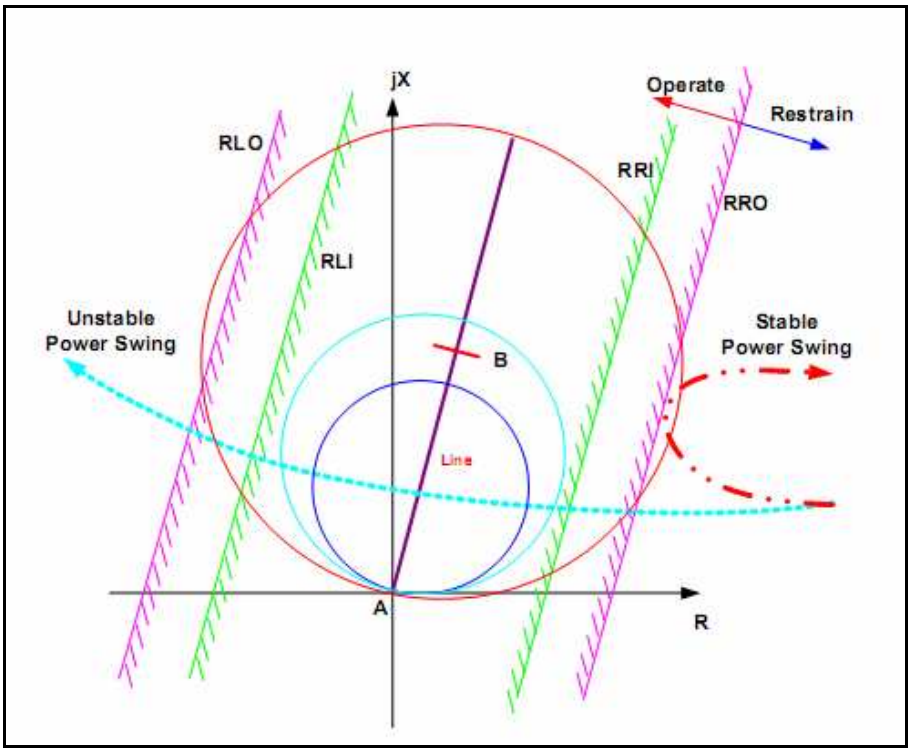

Figure 3.7: Two blinders scheme [2]

Operation principle depends on measuring the time taken by swing locus to traverse between outer and inner blinders. Blinders look to a certain direction. They are blind to the reverse swings and that is why they are named as blinders. Blinders are placed in pairs on left and right side of the origin.

If a power swing or fault causes the swing locus to cross the outer blinder, timer is initiated. Faults cause faster changes in R-X plane as compared to power swings. It can be pointed out that the movement is a sudden movement with generally less than 25 ms if a fault occurs. If the impedance locus does enter to the inner-blinder before a pre-determined time, PSB is not activated and short-circuit is decided by the relay. Line should be tripped depending on the zone set of the relay. If a power swing causes a movement of the impedance locus, traversing the inner and outer blinders will not be as fast as a fault. Blinders differentiate the power swing and trip-blocking is decided by the distance relay. It is possible to decide which protective zones of the distance protection will be blocked by PSB function.

3.3.2 Out-of-Step Tripping in Distance Relays

Movement of the impedance locus on R-X plane is not necessarily due to a fault. As angles change with respect to each other, swing locus follows a path on R-X plane which can traverse and completes a circular 360 degrees loop within a time interval depending on the slip frequency. An example of the movement of impedance locus following a system disturbance in a period of 60 seconds is shown in *Figure 3.8* [7]. One can trace the rectangular OST zones on the figure placed symmetrically around origin and how many times the complete cycle of slip is experienced.

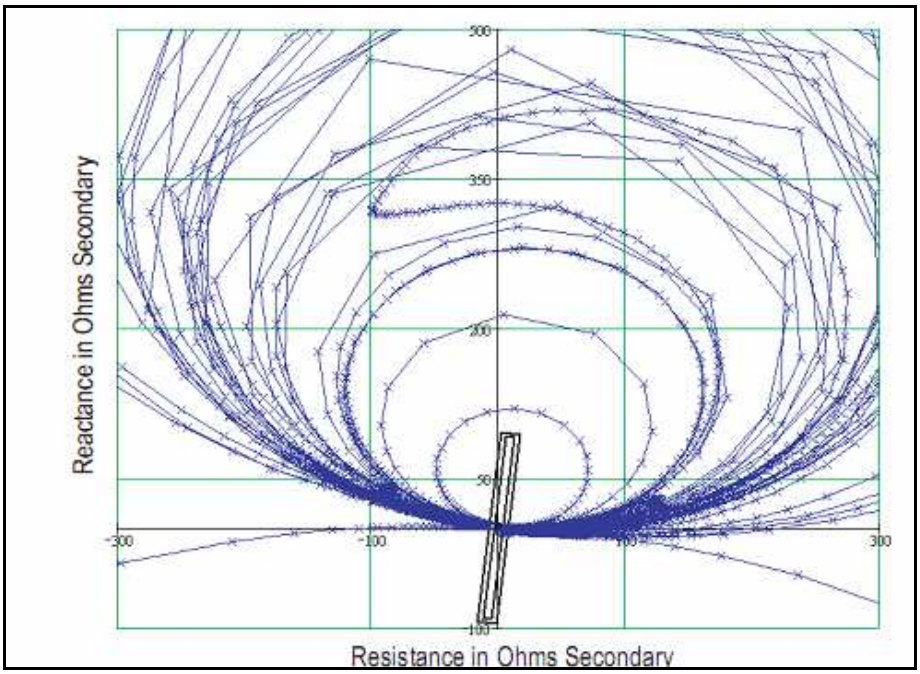

Figure 3.8: Impedance locus for a 60 second period following a disturbance

Although a power swing does not necessarily stem from a branch fault on the protective zone of a distance relay, one should distinguish between a stable and an unstable power swing and initiate the tripping action before a complete slip cycle is achieved between neighbour buses. Out-of-Step tripping is used to differentiate between stable swing which a system can recover itself and an unstable one which leads to complete pole slip for the buses.

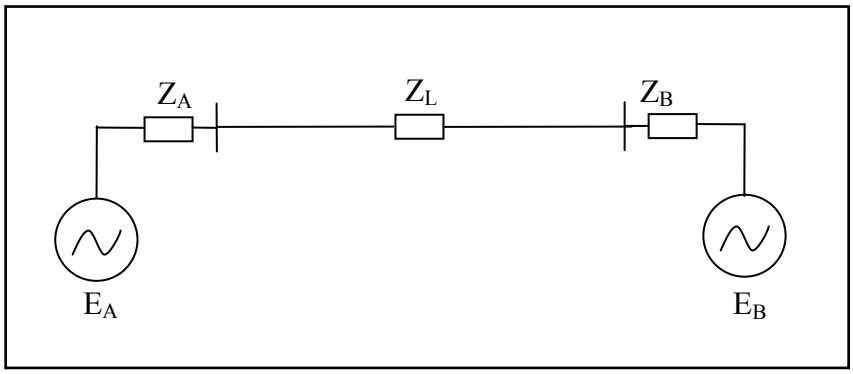

Figure 3.9: Two machine system

Out-of-step tripping is initiated when angles of consecutive buses differ by a certain critical angle. This angle defines the boundary between stable and unstable swing condition. Theory is best visualised on R-X plane for the two m/c system (*Figure 3.10*) [7].

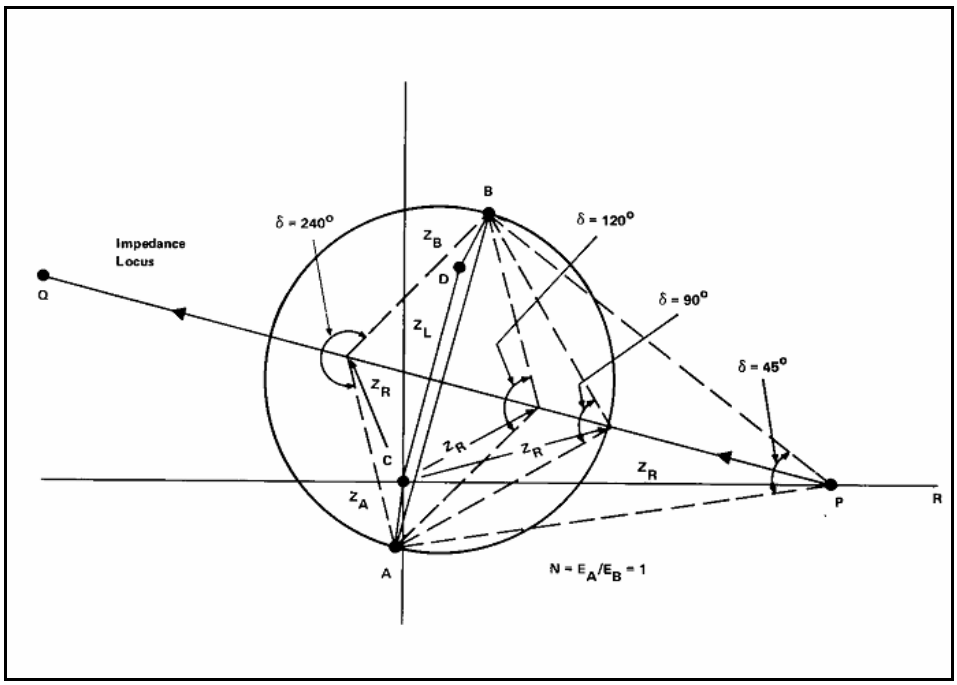

Figure 3.10: Swing locus for E_A/E_B=1

Circle in the diagram refers to $\delta=90^0$ point, where impedance measured by the relay equals to line impedance (i.e. $Z_R=Z_L$). Also, this is the maximum power transfer case by referring to *Eqn 2.12*. Out-of-Step boundary is determined by

detailed dynamic simulations and needs careful investigation. Calculation details are not in the scope of this study and explained in detail in [7] and [8].

Swings that cause undamped oscillations and lead to an instability are called unstable swings. An unstable swing condition is generally named as an out-of-step condition. Throughout the context of this study, term, "out-of-step" (OOS) is generally used to refer to an unstable swing condition.

Some out of step schemes are designed to operate only after the synchronism is lost. Other schemes attempt to actuate before the first pole slip (180 degrees separation) at the maximum stable swing angle. However for the latter case, determining the critical angle for the advance of swing from stable to unstable is difficult to determine. The critical angle and the resulting impedance trajectories are not fixed and differ dramatically as the fault location and system conditions vary [6].

3.3.3 Defining Parameters for OST Function

The best way to determine the critical OOS angle is to model the system using a transient stability program. The system representation must include all loads, generators, their voltage regulators and governor controls in a large area. Then; overall power system would be tested by applying faults at various critical points, using maximum clearing times for the stable-unstable swing boundary. These faults must be applied at various load levels, generation levels and system configurations to determine the most severe survivable swing.

In the absence of transient stability data, a general assumption is made that angular displacement beyond 120^o is not recoverable [5]. Out of step protection must be set to initiate a tripping action when the impedance loci exceed this value. Modern relays recommend 120^o adjustment as a rule of thumb.

Graphical consideration of the swing loci should consider the location of 120^o

and 240^{o} on the R-X plane. Both are required because a swing would traverse the relay characteristic in either direction due to the direction of the power flow during a transient behavior, although power would probably flow in one direction for the steady state condition.

Arcing and possible arc-restriking probability on the breaker contacts may be probable when out of step condition is detected on a pre-determined angle. It is common practice delaying trip of the circuit breakers to a more probable angle to reduce stress on circuit breaker contacts.

CHAPTER 4

ELECTRICAL SIGNIFICANCE OF THE Z MATRIX

4.1 CONSTRUCTION OF THE BUS IMPEDANCE MATRIX

The bus impedance matrix (Z) is simply the inverse of the admittance matrix (Y). It is commonly used for fault studies.

Constructing the Z matrix is much more difficult than obtaining the Y matrix. There is a step-by-step method developed to construct the Z matrix [9] but when large scaled power systems are considered, this method can be seen as time consuming one by hand calculation. However, this step-by-step algorithm is very suitable to construct the Z matrix by a programming language.

By using the Z building algorithm, it is possible to integrate changing load conditions to the network but this also makes use of computational burden to the analyzer. However, changing load conditions can easily be integrated as additional shunts to Y matrix by addition to the diagonal elements corresponding to that specific bus. Y matrix includes plenty of zero elements (sparse elements) which decrease the computational burden in some analysis like load flow analysis. Since Z matrix is the inverse of the Y matrix as mentioned above, impedance matrix can also be obtained by inversion of admittance matrix. However for some critical conditions termed as ill-

conditioned Y-matrices in the literature, it is much likely to get incorrect Z-matrices leading to difficulty in matrix inversion, especially for larger networks.

In this thesis work, Z matrix of the network was calculated by just inverting the Y matrix constructed manually from load flow data. Inversion is performed by the help of MATLAB software. In order to avoid the computational errors which may cause with the ill-conditioned complex Y matrix formation, Z matrix is found with the inversion of Y is validated with $\vec{Y} \times \vec{Z} = \vec{I}$ condition.

Y matrix gives detailed information about the shunt branches connected to a specific bus. However, physical significance of the elements of the Z matrix is much more difficult to distinguish by simple observation.

4.2 ELEMENTS OF IMPEDANCE MATRIX

The impedance matrix of a power system contains much useful but unrevealed information [10]. It is extensively used in short circuit calculations[11], determining the protective zones of the relays[12] and contingency analysis [13]. So, the physical significance of the Z matrix elements is worth to be discussed briefly in here.

The diagonal elements are the impedances existing between the buses in question and the ground. Namely, diagonal elements give the Thevenin impedances of the specific bus. This property makes use of the Z matrix in short circuit capacity calculations of the network buses. Also in most of the dynamical network reduction techniques developed, diagonal elements of the Z matrix are used to equivalence the rest of the network from the other parts.

The off-diagonal elements (Z_{jk}) correspond to the mutual impedances that exist between two buses. Z_{jk} is the voltage that will exist on bus "j" for a current of 1 p.u. flowing into (injected to) the other bus "k" with all other bus currents are

taken zero. Also, when other currents are taken zero, i.e. rest of the system is open-circuited, off diagonal elements are used to compute the voltage levels of the faultless buses by using only the current of the faulted bus. That is why, Z matrix elements are commonly defined as *Open-Circuit* parameters. They give information about the participation of a specific bus current (k^{th} bus) to the voltage of bus "j". Thevenin impedance between any two buses j and k can be calculated using the Z_{bus} entities as;

$$Z_{Th,j-k} = Z_{kk} + Z_{jj} - 2Z_{jk} \tag{4.1}$$

In order to visualize the points discussed above, Z matrix of a 2 machine system in *Figure 4.1* is given.

Z_A and Z_B are source impedances and Z_L is the impedance of the transmission line between two machines.

$$Z_{bus} = \begin{bmatrix} (Z_B + Z_L) // Z_A & \dfrac{Z_A . Z_B}{Z_A + Z_B + Z_L} \\ \dfrac{Z_A . Z_B}{Z_A + Z_B + Z_L} & (Z_A + Z_L) // Z_B \end{bmatrix} \tag{4.2}$$

As can be seen here, off diagonal elements include data about the neighborhood of the impedances. By generalizing the discussion to a more complex network, off diagonal values identify the links between two buses even if these buses are not directly connected, but instead, connected implicitly within the mesh structure of the power system. Implicit neighborhood of the buses which are not connected physically is not included in Y matrix since off-diagonal Y matrix elements are all zero. But when power system gets more complex, linkage identified by the off-diagonal elements of the Z matrix also become complex and difficult to visualize.

However, diagonal elements of the Z matrix are readily used in short circuit

calculations and have an explicit physical validity as defining the Thevenin impedances of the buses. Two buses physically connected by a transmission line can be shown simply as a reduced two machine network like the one in *Figure 4.1*, Z_L showing the actual impedance value of the transmission line connecting two buses. Off-diagonal elements corresponding to these two buses are in the same form as the ones of the 2 by 2 matrix given above.

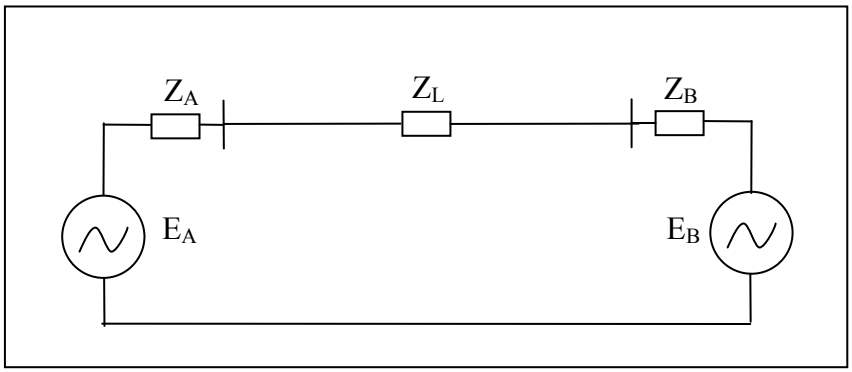

Figure 4.1: 2 machine system

Equality (or similarity) of the two terms $(Z_B + Z_L)//Z_A$ and $(Z_A + Z_L)//Z_B$ is dependent on the values of Z_A, Z_B and Z_L. By the use of symmetry, cases available for the values of diagonal elements are discussed below.

1) If $Z_A >> Z_B$, Z_L (or the same for Z_B),

$$Z_{bus} \approx \begin{bmatrix} (Z_B + Z_L) & \frac{Z_A.Z_B}{Z_L} \\ \frac{Z_A.Z_B}{Z_L} & Z_B \end{bmatrix} \tag{4.3}$$

Similarity of the diagonal elements is dependent on the similarity of Z_B and Z_L values. If Z_L is small, two values are very close. If Z_L is large compared to Z_B, two diagonal elements are apart from each other.

2) If $Z_A << Z_B$, Z_L (or the same for Z_B),

$$Z_{bus} \approx \begin{bmatrix} Z_A & \dfrac{Z_A.Z_B}{Z_B + Z_L} \\ \dfrac{Z_A.Z_B}{Z_B + Z_L} & Z_L // Z_B \end{bmatrix} \tag{4.4}$$

Similarity is not expected in this case. Two off-diagonal values are greatly far from each other.

3) If $Z_L >> Z_A, Z_B$

$$Z_{bus} \approx \begin{bmatrix} Z_A // Z_B & \dfrac{Z_A.Z_B}{Z_L} \\ \dfrac{Z_A.Z_B}{Z_L} & Z_A // Z_B \end{bmatrix} \tag{4.5}$$

In terms of a distance measure, two diagonal elements are very close to each other, when shown as separate data parts in real-imaginary euclidean space. Closeness is not dependant on the values of Z_A and Z_B.

4) If $Z_L << Z_A, Z_B$

$$Z_{bus} \approx \begin{bmatrix} Z_A // Z_B & \dfrac{Z_A.Z_B}{Z_A + Z_B} \\ \dfrac{Z_A.Z_B}{Z_A + Z_B} & Z_A // Z_B \end{bmatrix} \tag{4.6}$$

Two elements are also very close to each other. Closeness is not still dependent on the separate values of Z_A and Z_B as in case 3.

As shown in cases 3 and 4, when transmission line impedance value (Z_L) differs gradually from that of the machines (Z_A and Z_B), diagonal elements of

the Z matrix corresponding to these buses are very close to each other when placed in the euclidean space.

4.3 INTERPRETATION ON THE CLOSENESS OF DIAGONAL ELEMENTS

Observation of the closeness of the off-diagonal elements can be used to identify the strength of the transmission linkage between buses. Buses which are loosely connected to the rest of the system can be determined by analyzing the diagonals of the Z matrix entities.

If diagonal elements (i.e., the short circuit capacity) for the neighbor buses connected by a transmission line (of impedance Z_L), is very close to each other, it can be predicted that these two buses are connected strongly to each other. However if two neighbor buses have diagonal elements remarkably wide apart from each other as in case 2, it would be expected to have a weaker connection.

Theory to be tested in this thesis stems from the scattering of the diagonal entities of the impedance matrix. If two physically connected buses (neighboring buses) are placed to two separate clusters when partitioned by a data analysis method, transmission line connecting these two buses is referred to be a weaker connection than the ones connecting two buses placed in the same cluster. On the tie-line connecting these two buses it is more probable to encounter an out-of-step condition by the effect of the swings resulting from a power impact.

CHAPTER 5

DATA CLUSTERING APPLIED TO Z MATRIX

5.1 DATA CLUSTERING

Data clustering is an assignment of objects into groups so that objects in the same group are more similar to each other than the ones in the other groups. Groups are commonly referred as clusters. It is a collection of techniques of statistical data analysis which is used in many fields like bioinformatics, image processing, pattern recognition and data mining. Similarity between data points is estimated according to a distance measure. Measure of the similarity defined is dependant on the application.

There are many clustering methods available, and each of them may give a different grouping of the same dataset. Depending on the application, suitable method and hence clusters formed may differ. Clustering algorithms may be classified in the taxonomy given in *Figure 5.1*.

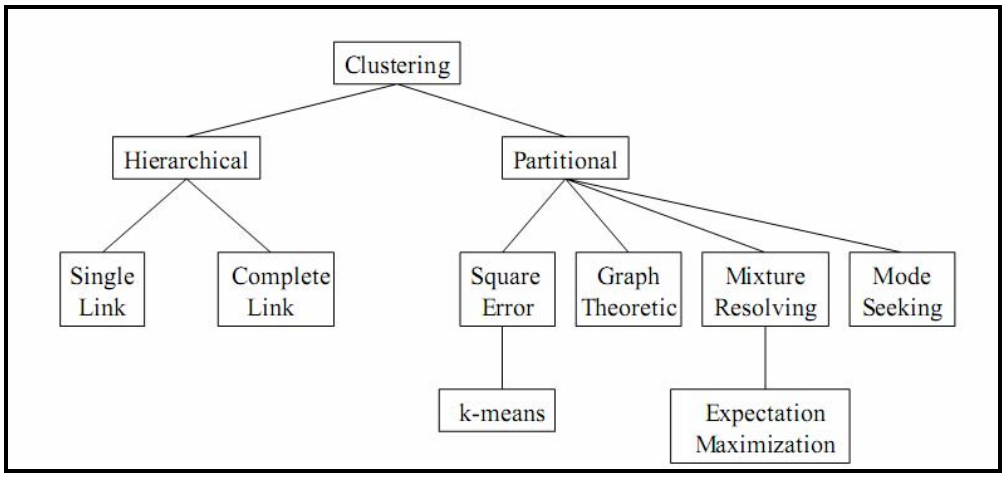

Figure 5.1: Taxonomy of different clustering approaches [10]

There is a distinction between Hierarchical and Partitional approaches. Partitional algorithms allow partitions containing single data to be formed whereas hierarchical algorithms may give rise to nested partitions containing multiple data in later steps. Detailed analysis of the different clustering techniques is out of the scope of this thesis. Two basic methods; k-means clustering and hierarchical clustering will be briefly introduced here.

5.1.1 Hierarchical Clustering Method

The hierarchical agglomerative clustering methods are most commonly used. Given a set of N items to be clustered, and calculating an N*N distance (or similarity) matrix, the construction of a hierarchical agglomerative classification can be achieved by the following general algorithm.

1. Find the 2 closest objects and merge them into a cluster.
2. Find and merge the next two closest points where a point is either an individual object or a cluster of objects.
3. If more than one cluster remains , return to step 2

Hierarchical clustering groups data over a variety of scales by creating a cluster tree or dendrogram. The tree is not a single set of clusters, but rather a multilevel hierarchy, where clusters at one level are joined as clusters at the

next level. This allows deciding the level or scale of clustering that is most appropriate for the application. Namely, one can decide where to stop clustering.

Method is best visualized by an example containing 7 data points in *Figure 5.2*. At the beginning each data point is treated as a separate cluster. Data points form groups according to the maximum similarity (minimum metric distance) between them. In each step only one grouping is performed. But every formed cluster, which can be a combination of more than one data, is treated as a separate cluster in new step.

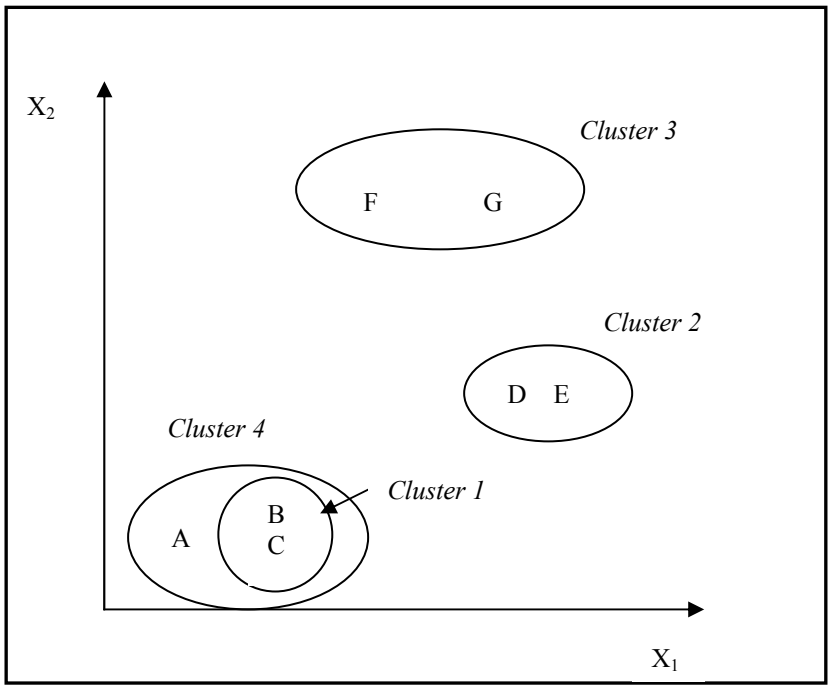

Figure 5.2: Points falling in first 4 clusters.

Maximum step number of the clustering process can be defined in hierarchical clustering method. If otherwise stated, clustering ends when all data groups are integrated in one global cluster. Clustering steps are shown on a diagram referred as dendrogram (*Figure 5.3*). A dendrogram consists of many U-shaped lines connecting objects in a hierarchical tree. The height of each U represents

the distance between the two objects being connected.

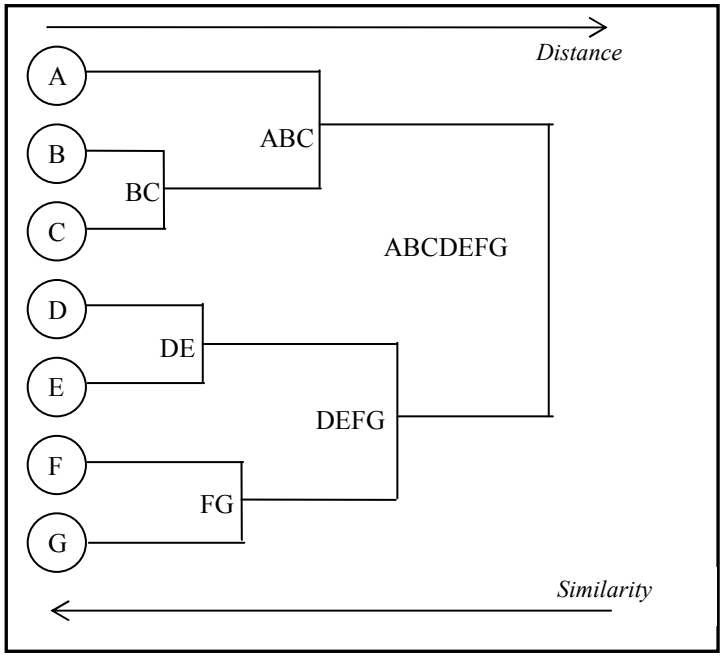

Figure 5.3: Dendrogram formed for the example

By using the pair-wise distances of the separate pairs of data, an *N* by *N* distance matrix *D* is formed. Distance matrix is a symmetrical square matrix with zero diagonals composed of distance elements (commonly Euclidean distance) d_{ij}'s as in *Eqn 5.1*.

$$d_{ij} = \sqrt{(x_i - x_j)^2 + (y_i - y_j)^2} \qquad (5.1)$$

Distance is measured with different methods. In single linkage method, distance between two clusters is considered to be equal to the shortest distance from any member of one cluster to the any member of the other cluster whereas distance is considered as the greatest distance in complete-linkage method and average distance of the separate members of the cluster is taken into account in average-linkage method.

Distance matrix is modified in each step by deleting the rows and columns of the elements forming new cluster and adding new row and column corresponding to the new cluster formed. Data points with minimum d_{ij} of the new *N-1* by *N-1* matrix are chosen to form the preceding cluster in the

upcoming step.

5.1.2 Partitional Clustering Method

A partitional clustering algorithm obtains single partition of the data in each step of the algorithm in contrary to nested clusters formed in later steps of the hierarchical algorithm. They are known to have advantages in partitioning large data sets and tracking a separate data point within the final clusters since the dendrogram formed in hierarchical methods as in *Figure 5.3* or distance matrix become complex for large numbers of data. However, optimum number of desired output clusters to be formed is difficult to decide. In practice, algorithm is applied many times with different starting states to be on the best side.

K-means clustering method is known to be the most widely used partitional clustering algorithm in the literature [14]. Algorithm starts with the choice of the number of partitions to be formed.

1. Form initial partitions around randomly placed centroids.
2. Assign each data to the closest centroid.
3. Compute new centroids of the partitioning. Reassign partitions around new centroids.
4. Continue until a pre-defined convergence criterion is met. Convergence is achieved when centroids no longer move considerably.

The most used convergence criterion is the squared error term in *Eqn 5.2* measuring the square of the distance between each data and centroid.

$$e^2 = \sum_{j=1}^{K} \sum_{i=1}^{n_j} \left\| x_i^{(j)} - c_j \right\|^2 \qquad (5.2)$$

Here, $x_i^{(j)}$ defines the data points belonging to the j^{th} cluster and c_j is the centroid of the j^{th} cluster.

Major drawback of the k-means method is that depending on the initial choice of partitioning, resultant clusters to be formed may differ significantly. Error

value may converge but obtaining a global minimum error needs several trials with different initial guesses which is computationally prohibitive [9].

In the example presented before for 3 cluster formation, initial placement of the centroids (squares) in the left case of *Figure 5.4* results the partitioning as {[A]; [B,C]; [D,E,F,G]} whereas a correct initial guess in the left case will yield more graph-oriented partitioning result as {[A,B,C]; [D,E]; [F,G]} achieving the minimum error term.

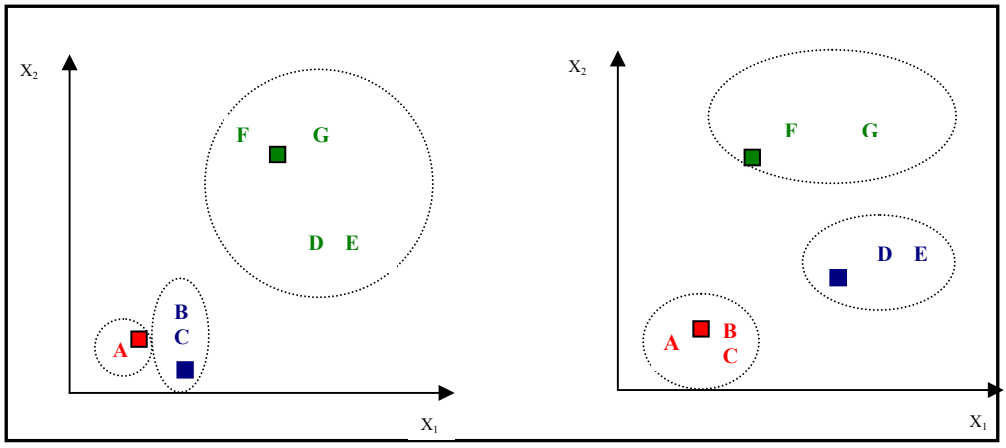

Figure 5.4: k-means clustering applied for different initial centroids attained

5.2 OVERVIEW OF IEEE 39 BUS TEST SYSTEM

IEEE 39 bus system is a dynamical test system including 10 synchronous generators equipped with exciters *(Figure 5.5)*. It is known to represent the actual power system of New England in 1960's. Actual data is known to be published in an old study report which is out of print [15]. A paper of Athay et. al. [16] is said to be serving the data of the original report in 1979.

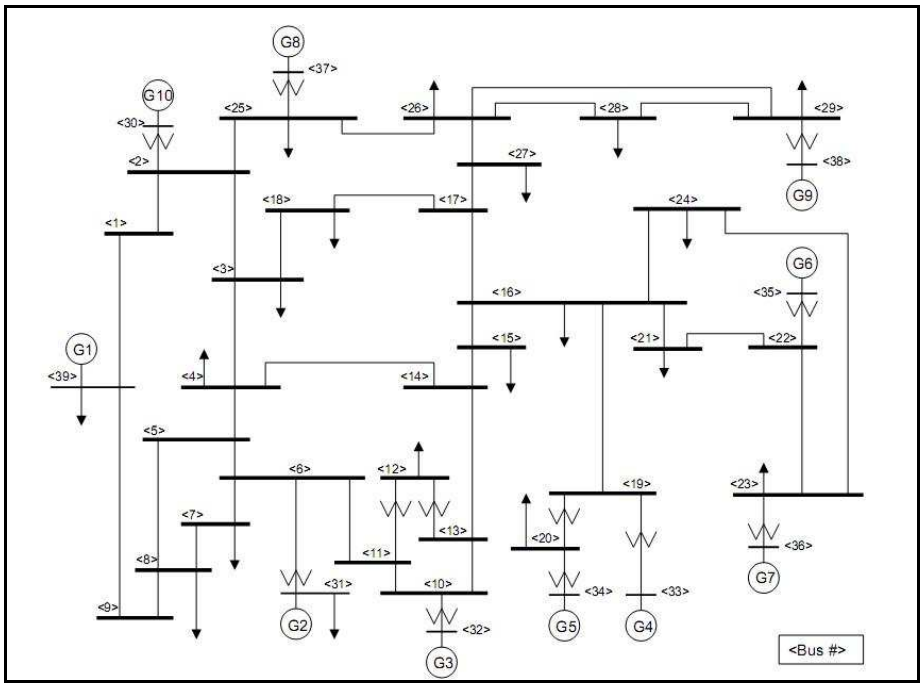

Figure 5.5: New England Test System

Generally accepted version of the system data can be obtained from [17]. In this thesis, static and dynamic data is taken from [18]. Minor discrepancies exist between the data in [17] and [18], especially on power factors of the loads. At buses 7 and 16, Q values of the loads are 10 times the originals in [15]. However, this does not lead to a catastrophic problem in the scope of the study conducted here, and hence data are directly taken from [18].

This system can be referred as sufficiently large to test and explain the dynamic power system behavior. Results can be generalized to common power system behavior since system is equipped with loads, generators, transformers and lines distributed within the mesh structure of the network as in up to date power systems. Additionally, system is not too large to be mistaken when investigating the correlation between different power system quantities and to dig into time-consuming analysis of the results.

Governors are not available in the version of the system data used. As the simulation period used in this study is limited to 2 seconds, it is not expected to

get a mechanical governor action within the period under investigation by looking at the default values of actual governor time constants.

As experienced in later steps of the thesis, New England Test System is a rather stable system with strongly connected transmission links. Most of the buses are connected to the rest of the system with more than one branch, blocking the formation of islanded parts in case of a single line tripping.

Automatic high-speed reclosure is known to be a widely used measure against power swings in HV networks. In the working group report of CIGRE, automatic high-speed reclosure is reported to be one of the most widely used measures taken (68%) against out-of-step adopted at power system planning [19]. However, it is very difficult to disturb the stability of the New England System with a single fault following the reclosure of the faulted branch. Fault duration in this study is increased in steps by checking the relative machine angles. By increasing the fault duration, magnitude (or the severity) of the power impact is increased as explained in Chapter 2. It is aimed to obtain two or more groups of machines whose angles are separating from each other in different directions in order to decide the disturbed stability of the system after a specific fault.

Fault durations leading to out-of-step conditions in the system are in the order of 0.4-0.6 seconds which corresponds to 20-30 cycles in 50 Hz basis. They may not seem to be realistic when tripping of the protective relays in their first operating zone is considered, however; increase in the fault duration is needed in order to pull the system out of step. Intensity of the power impact caused by the fault is magnified by adjusting fault duration in the simulations performed.

5.3 STATISTICAL METHODS IN POWER SYSTEM ANALYSIS

As well as in other branches of science, amount of data available in power system field is exponentially increasing from the beginning of the application of digital measurement and data storage techniques. As the amount of data is

increased, many methods of processing these vast data are invented. Available data is used in many aspects to give an understanding of the nature of some common power system behaviors.

Data mining aims to extract useful information from large databases. Useful methods of statistics and increased capabilities of machine learning are integrated to get the use of data mining applications in power system field. Classification, clustering, association rules and regression analysis are four basic methods used in data mining.

Data mining techniques are employed in many sub-fields up to now when power system analysis is concerned. These sub-fields ranges from transmission system planning[20], power quality disturbance monitoring[21], load forecasting[22] to reliability issues, automatic generation control (AGC)[23], protection equipment[24], pollution flashover fault forecasting [25], load forecasting and much more.

Detailed report of CIGRE is available discussing the data mining methods applicable to power system field [26].

5.4 HIERARCHICAL CLUSTERING APPLIED TO Z MATRIX

In the context of this study, hierarchical clustering method briefly introduced in chapter 5.1 is used to classify the buses in the sample test system introduced in 5.2.

First, admittance matrix (Y_{BUS}) of the network is obtained from the load flow solution data. Y_{BUS} is inverted to obtain impedance matrix, i.e. Z_{BUS} of the sample test system.

Difficulty can be faced for the numerical matrix inversion techniques for some cases with ill-conditioned matrices as introduced in the literature [27].

Condition $Y_{BUS}.Z_{BUS}=I$ where I is identity matrix, is verified for that reason.

Diagonal entities of Z matrix is used to form clusters according to hierarchical clustering algorithm. Diagonals matrix *DIAG* of size 1 by 39 is formed which includes diagonal entities of Z bus in vector form as listed in the appendix section.

Then a distance matrix *DIST* is formed which includes the pairwise euclidean distances for each element of *DIAG.* Namely; *DIST* is a 39 by 39 square matrix with all diagonal entities zero. *DIST* consists of elements such that

$$dist_{ij} = \sqrt{((x_i - x_j)^2 + (y_i - y_j)^2} \qquad (5.3)$$

At first, all elements form one global cluster as in *Figure 5.6.* Real axis of the graph is multiplied by 10^{-3}, which may cause an improper scaling about the distances at first. However horizontal distances between elements are very small compared to vertical ones. Some elements are labeled with their bus number for the reader to follow the results easily.

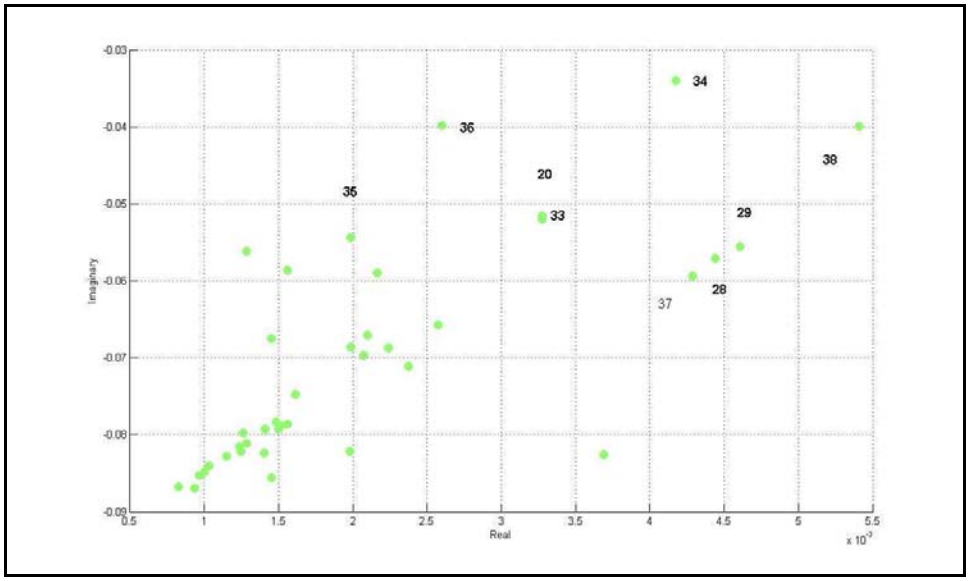

Figure 5.6: Diagonal entities of Z_{BUS} for IEEE-39 bus test system

5.4 CLUSTERS FORMED IN IEEE 39 BUS TEST SYSTEM

All separate elements are treated as a separate cluster at the beginning of the clustering algorithm. In the first clustering step, maximum pairwise distance for i≠j is chosen as the farthest element which will form the first multi-element cluster of the algorithm. Rests of the elements are still treated as separate clusters for the first clustering step. Now, a new distance matrix *DIST* of size 38 by 38 this time is calculated for the second step of the clustering. First cluster is treated as a separate and one distinct element for the upcoming steps of the algorithm. At each step, a modified distance matrix *DIST* of size (39-n) by (39-n) should be calculated for which n equals to the clustering step, i.e. loop-count in the algorithm.

Clusters formed in some steps of the algorithm are given in *Figure*s *5.7, 5.8* and *5.9.* Elements belonging the same cluster are shown with the same color in the graph.(This may not seem to be visible in black and white print)

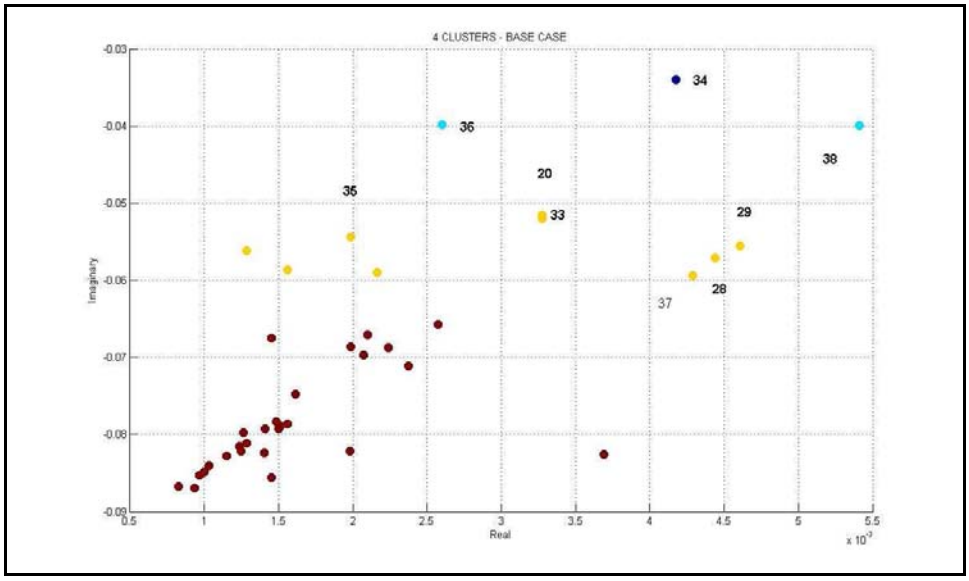

Figure 5.7: 4 clusters formed

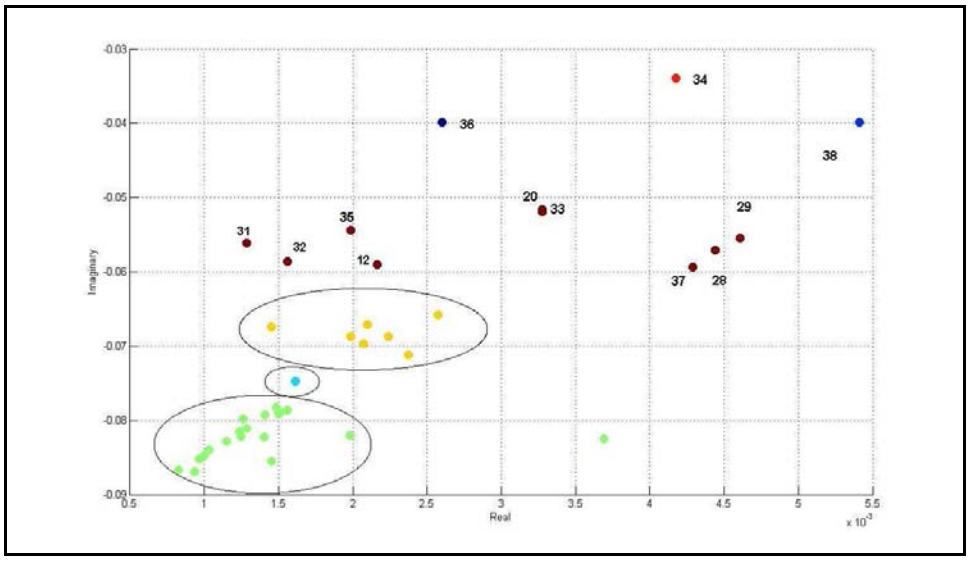

Figure 5.8: 7 clusters formed

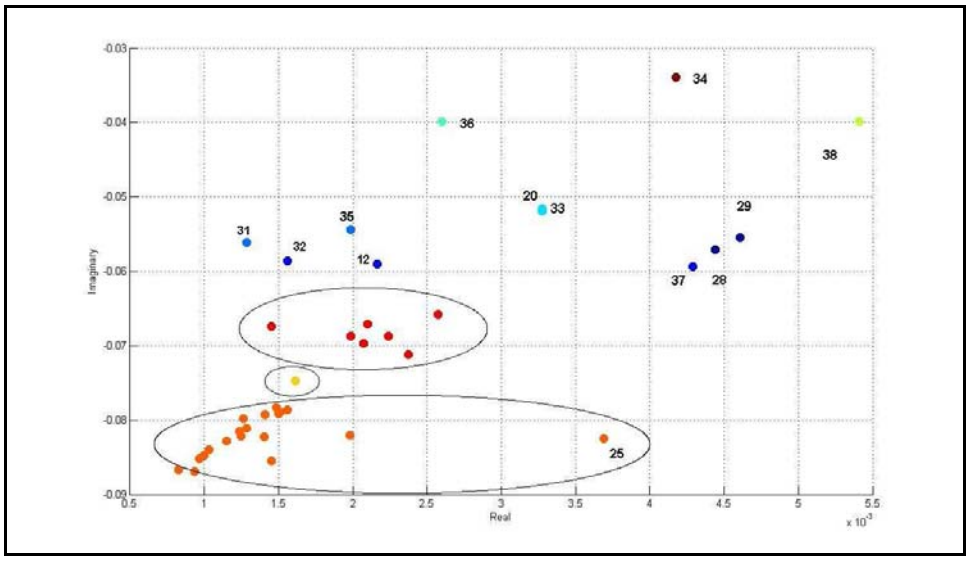

Figure 5.9: 10 clusters formed

CHAPTER 6

SIMULATIONS ON THE TEST SYSTEM

6.1 METHODOLOGY

6.1.1 Simulation Methodology

Simulations are performed on IEEE 39 bus test system. Test system is introduced in chapter 5 of this study.

PSS/E software is used in dynamic simulations. Faults are applied on specific buses in order to create meaningful power swings. Simulation step time is chosen as delta=0.001 seconds.

Simulation output variables are printed with incremental time step of $\Delta t=0.01$ sec. to reduce output file size and to ease tracing.

6.1.2 Evaluation of Simulation Outputs
(Relay 0.85 p.u. Axis Method)

Relays process impedance measurements in ohm basis. Each line has its own impedance value in ohms.

Impedances seen by the relays located at the beginning terminal of each line are printed as simulation output by PSS/E. Original output values are magnitudes of the R and X values read by the relays in ohms.

In practice, distance relays are adjusted to trip in their instantaneous operating zone when 85% of the line impedance is reached. Left 15% margin is due to the possible measuring errors of equipment transformers and line impedance data as explained in chapter 2.

In context of analyzing simulation outputs, R(t) and X(t) of each line are used to find Z(t) (impedance) magnitude monitored by relays. In order to be more clear and to give a comparison view on the same basis, Z(t) is divided by the real total Z value of each line (i.e. Z_{Ljk} of each line) to transform p.u. form. Total line impedance is equivalent to 1 p.u. for all lines. This makes easier comparison when relay outputs are viewed on the same graph. Line reaching 0.85 p.u. value (on its own base) can be considered as to reach the tripping area of the possible distance relay on that line and will immediately be tripped if tripping is not blocked or transferred.

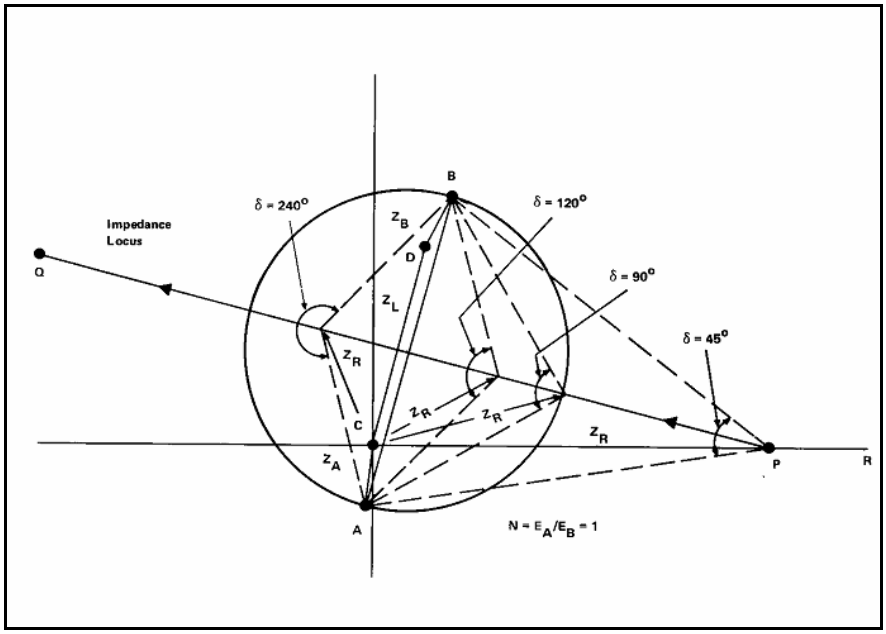

Figure 6.1: Swing locus for EA/EB=1

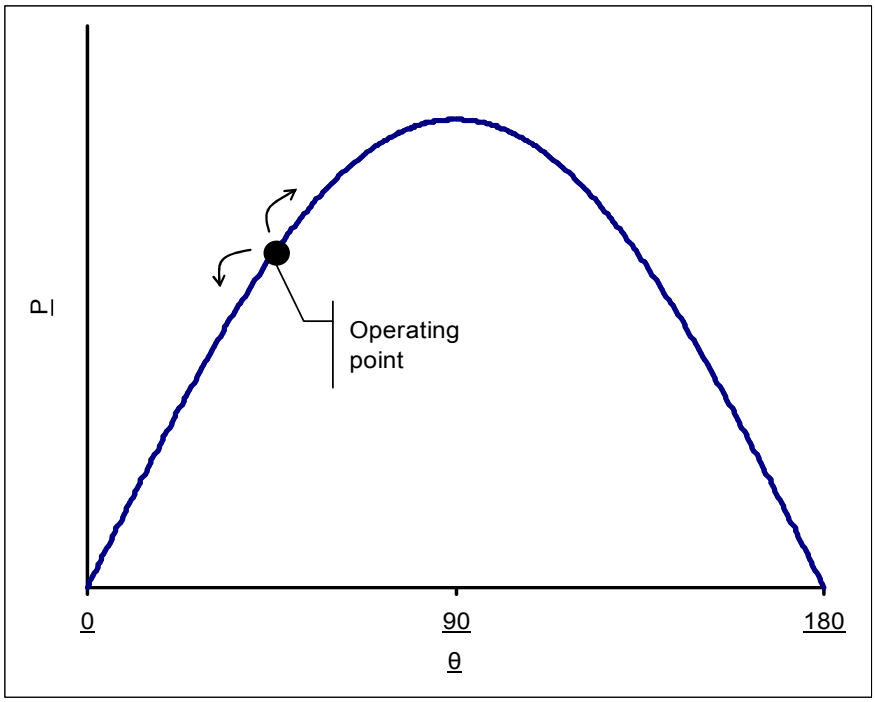

Figure 6.2: Swing Curve

Figure 3.10 is again presented here as *Figure 6.1* for the convenience of the reader. As briefly introduced in Chapter 2, impedance loci travels through the path in *Figure 6.1* when bus angles change with respect to each other. In addition, power transfer between buses is moving on the well known swing curve in *Figure 6.2* simultaneously with impedance loci.

Circle on *Figure 6.1* refers to the region when impedance of the operating loci equals to line impedance value. ($Z_{Relay}=Z_{Line}$) This point also corresponds to $\theta=90^0$ point on the swing curve that is the maximum power transfer point. Angle θ is angular difference between voltages E_A and E_B.

As explained in Chapter 2, out-of-step protection function is employed in modern distance relays to differentiate stable swings which system can recover from unstable swings. Setting the stable-unstable boundary needs very detailed dynamic analysis of the overall system so, a practical 120^o assumption is used. System is assumed not to regain stability again when angular difference

between bus angles exceeds 120^o. Note that sin (120^o) =0.86 which is very close to instantaneous fault-trip region of the distance relay.

Out-of-Step boundary is chosen as $\theta=90^0$ point in the study of Adibi *et. al*. [28]. Although, $\theta=90^0$ point is peak-point of power transfer curve, system can recover itself for points above $\theta=90^0$ point depending on system topology as can be proved with Equal-Area Criteria. Details can be found in Chapter 3.

The general assumption accepted in this study is such that stable-unstable swing boundary is equivalent to 120^o angular separation between buses. That is why 0.85 p.u. is used as an indicative of Out-of-Step condition when analyzing simulation outputs. ($Z_{Relay}=0.85.Z_{Line}$)

6.1.3 Case Introduction and Result Format

Theory will be tested by means of simulations. Each simulated case aims to explain different sub-theories which will then sum-up to general conclusions at the end.

Details of cases will be presented on a *Case ID card* shown in table format. In order to visualize things, case details like fault location, relay positions and relay directions will be shown on a *case-layout figure*. Relays are indicated as red boxes on case layouts. Numeric case results will be given on a combined time graph to trace time-dependent changes. Some explanatory text-boxes are integrated on graphs for convenience of the reader. Some cases include R-X diagrams to visualize the out-of-step condition. Single R-X diagram shows impedance oscillations of one line only.

6.2 PROCEDURE

It is stated in the literature [28] that **location of loss of synchronization (i.e., OOS line) is independent of location and severity (fault duration) of the initial fault**.

One should validate the statement mentioned above before proceeding to verify theory of this thesis. Effect of fault intensity and effect of fault location will be investigated at first.

6.2.1 Effect of Fault Intensity on OOS Order *(Case-C1 and Case-C2)*

First simulation aims to check if OOS occurrence order is dependent on fault severity or not. Fault severity is increased by increasing fault clearing time. Two separate faults with slightly different clearing times are simulated to test the statement.

Not all of the lines are investigated for this purpose. Three lines are checked for OOS sequence for this part of the study. These lines are chosen as slightly remote from fault location and placed in a radial path. Lines investigated and fault clearing times can be traced from *Figure 6.3*. Details of the cases can be traced from case identity given below in *Table 6.1*.

Table 6.1: Case Identity Card for C1 and C2.

Case ID	C-1	C-2
Fault Data	3-Phase Solid fault on one of Double LINES 15-16	
Fault initiated at (s) Fault period (s) Fault cleared at (s) Reclosure at (s)	0.1 0.1-0.5 0.5 0.75	0.1 0.1-0.6 0.6 0.85
Lines observed	Line 17-27 Line 26-29 Line 27-26	Line 17-27 Line 26-29 Line 27-26

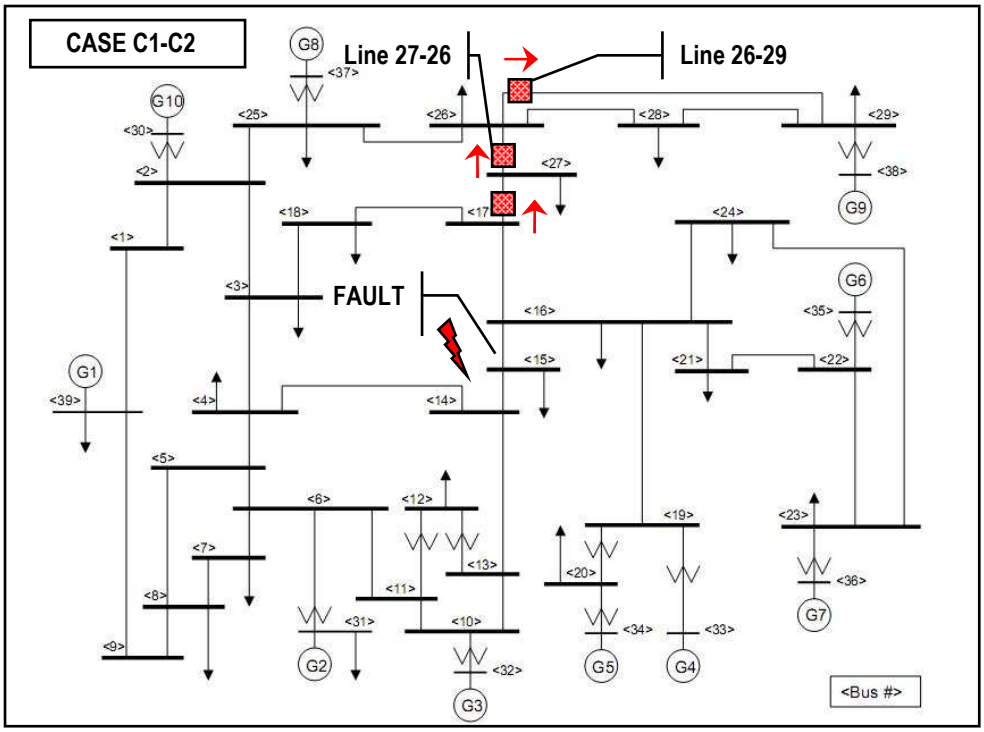

Figure 6.3: Layout of Case-C1 and Case-C2

Fault clearing times are adjusted so that all of the three lines have faced OOS condition (i.e., critical clearing times for all three lines are exceeded).

Case-C1

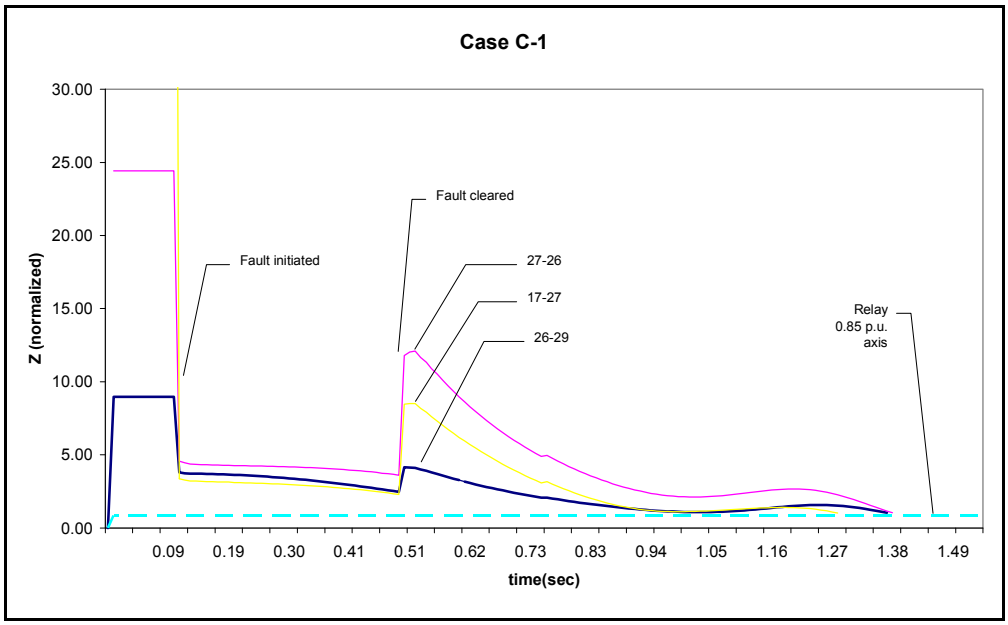

Figure 6.4: Line Impedance values and OOS order for case C1

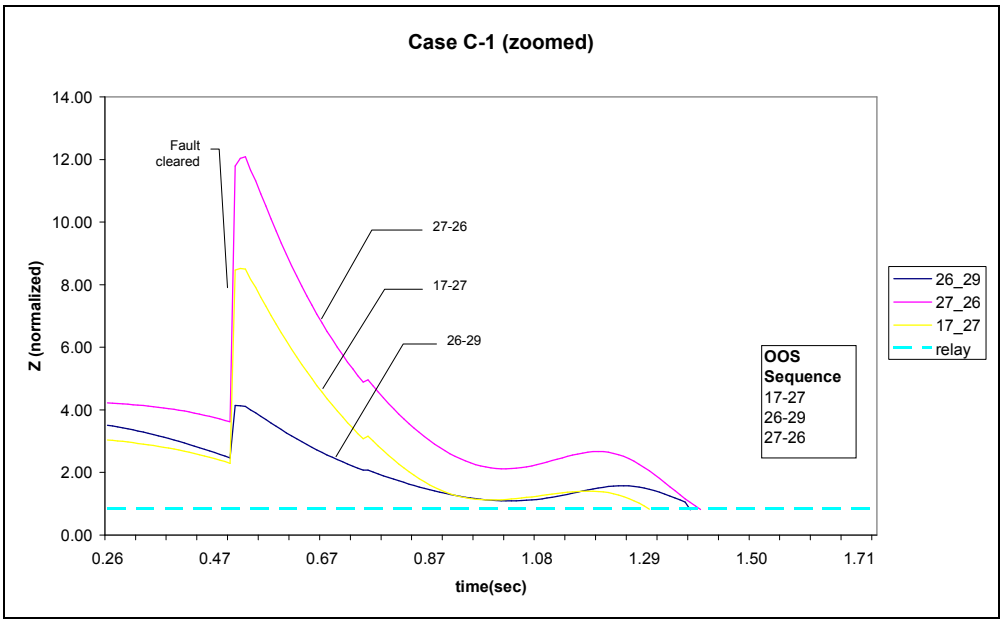

Figure 6.5: Zoomed view for C1.

Case-C2

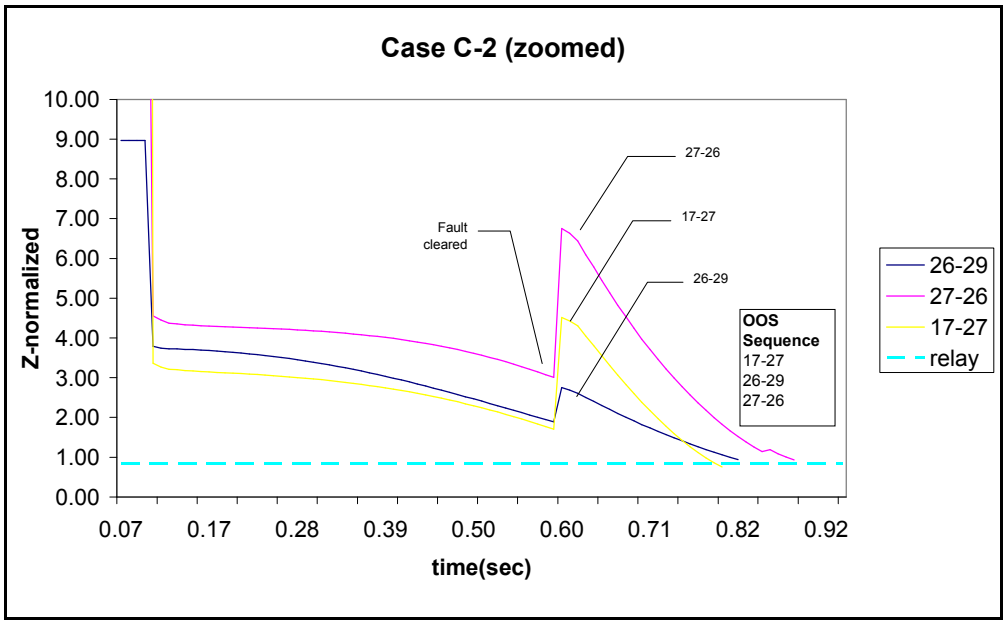

Figure 6.6: Line Impedance values and OOS order for case C2.

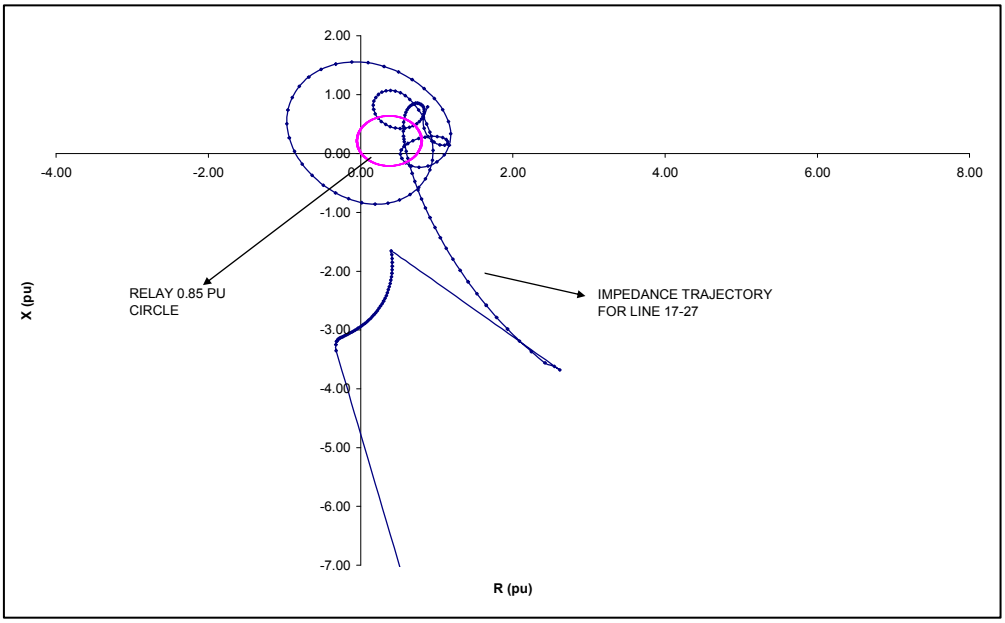

Figure 6.7: Impedance trajectory on R-X diagram for line 17-27 case C2.

As fault intensity is magnified, OOS sequence does not change between two cases; C1 and C2. This is not a general conclusion but can be generalized with different cases as stated in the literature. Also there is an interesting conclusion that must be pointed out. Line 26-29 which is physically the most remote line to the fault location among investigated three lines, comes second in OOS sequence.

Hence; two statements can be deduced from these two simulations.

1) Fault intensity does not affect OOS sequence.
2) OOS sequence is not dependent on physical closeness to the fault location.

Power impacts may be higher at remote lines from fault locations.

6.2.2 Effect of Fault Location on OOS Order

Second group of simulations aims to check if OOS occurrence order is dependent on fault location or not. Fault is applied to two different buses on two different cases. Fault clearing times are chosen equal to reduce effect of fault intensity. Note that, for different faulted buses, it is not completely possible to equalize fault intensities. There is not a distinct measure of fault intensity although it is partially dependent on clearing time.

Case details can be traced from case ID card on Table 6.2.

Table 6.2: Case ID card for C3 and C4.

Case ID	C-3	C-4
Fault Data	3-Phase Solid fault on LINE 15-16	3-Phase Solid fault on LINE 3-4
Fault initiated at (s)	0.1	
Fault period (s)	0.1-0.45	
Fault cleared at (s)	0.45	
Reclosure at (s)	No Reclosure	
Lines observed	Line 2-1 Line 9-39 Line 8-9 Line 29-38 Line 26-28 Line 22-35	

Case-C3

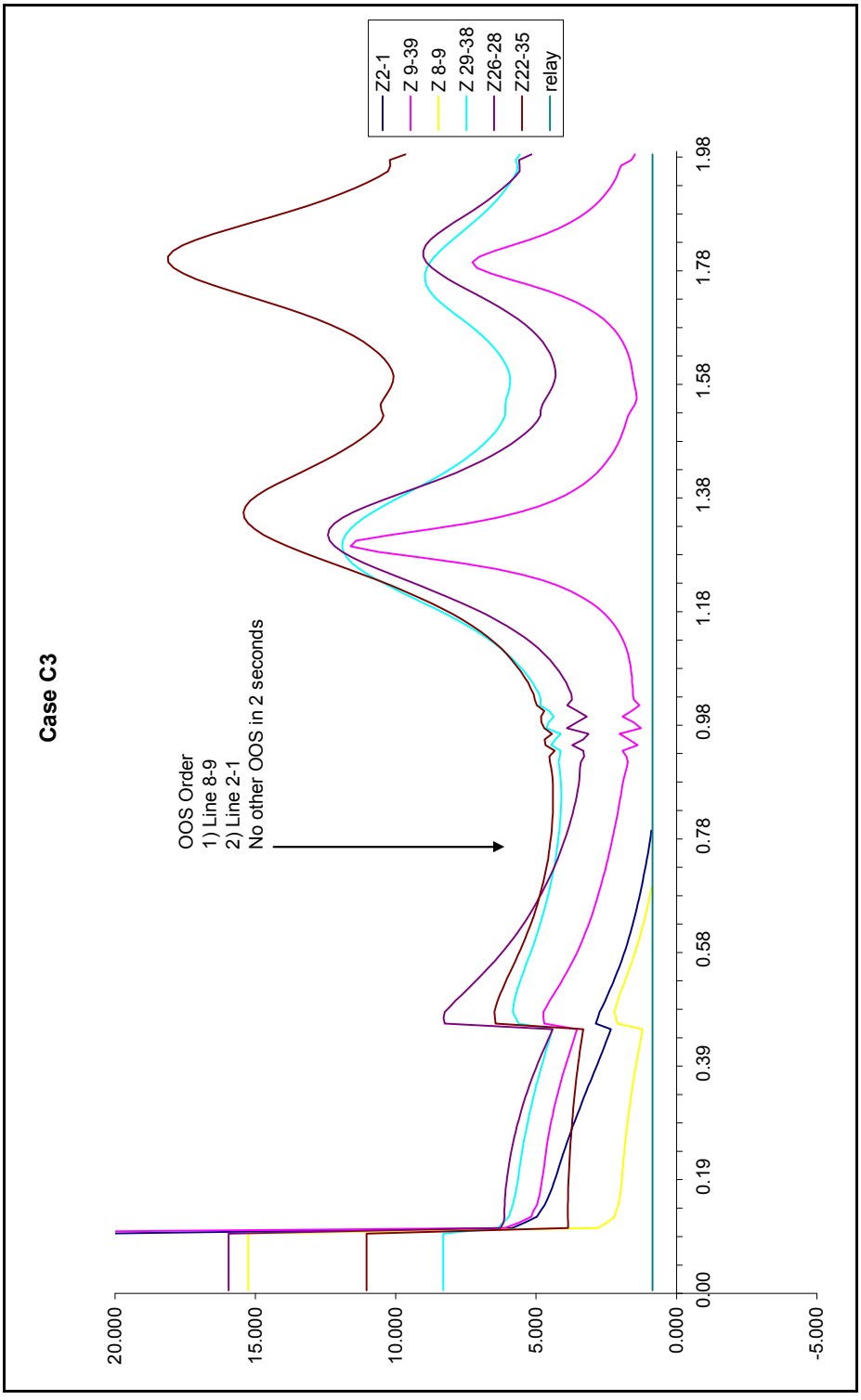

Figure 6.8: Line Impedance values and OOS order for case C3.

Case-C4

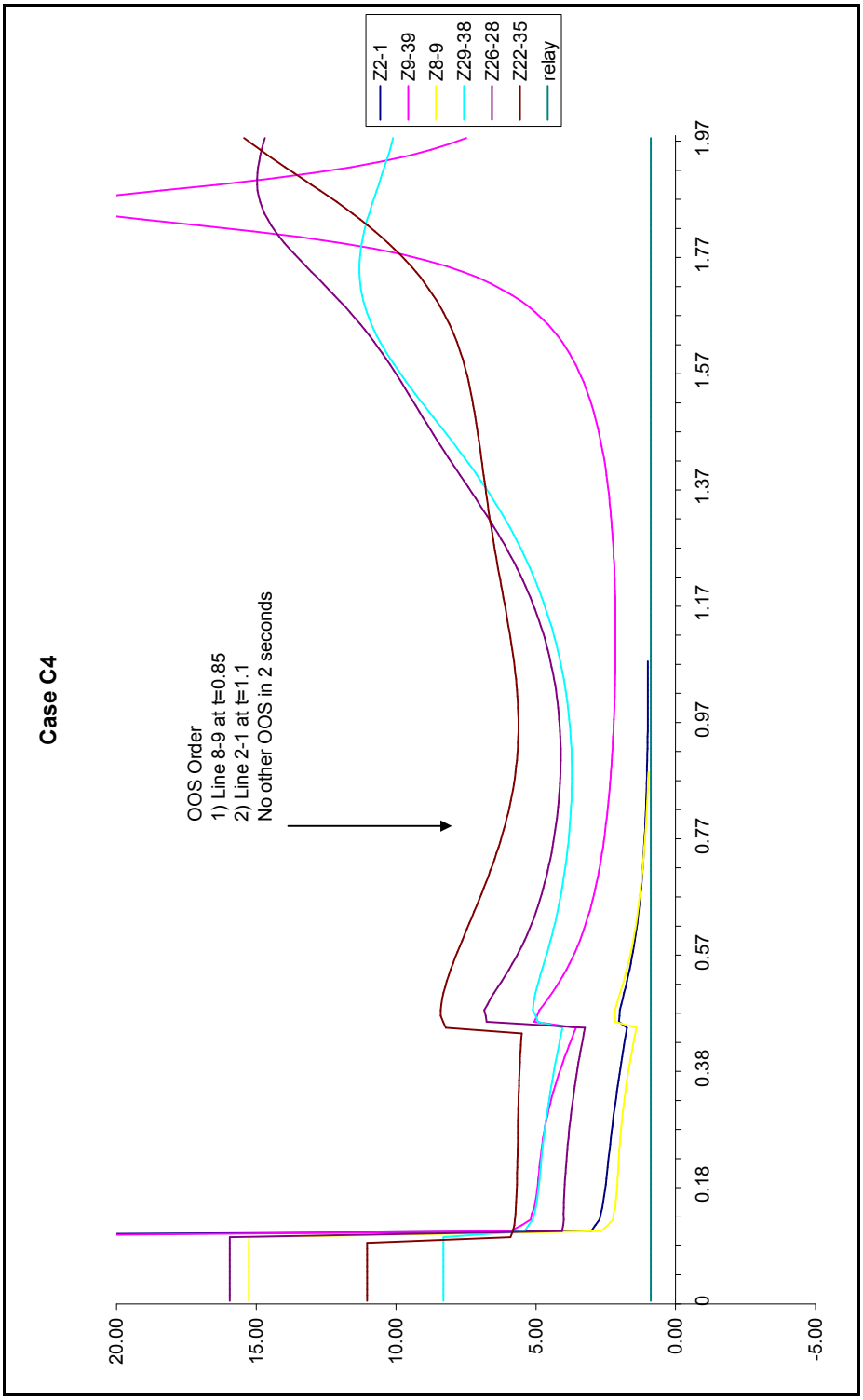

Figure 6.9: Line Impedance values and OOS order for case C4.

Two faults with same fault durations are applied to two different lines. Among the investigated 6 lines, OOS is occurred on two lines with the same sequence within the time period of 2 seconds. Line 8-9 is followed by line 2-1 in OOS sequence. Although OOS is delayed for the same line for two different fault locations, OOS sequence does not change.

It can be concluded from the second simulation that; fault location does not affect OOS sequence.

These two proven property make use of the general understanding that; whatever the fault severity and fault location is;

OOS is observed

i) On some weak links of the system

ii) In a pre-defined sequence.

Defining the weak links of the system is the main concern of the theory tested within the context of this thesis. Next section checks the sequence of OOS for cases C3 and C4 among all lines this time. But before the simulation, grouping of the buses according to the clusters formed in Chapter 6 is worth to introduce here.

6.3 CORRELATION BETWEEN OOS ORDER AND CLUSTERS

This part aims to define a correlation between OOS occurrence and bus grouping formed by cluster analysis in Chapter 5. Original IEEE 39 bus system is analyzed, and then, a simple modification is performed on the system topology. New clusters are defined and same type of a power impact is tested and results are compared for two system topologies.

It is better to define the bus groupings formed for the original test system, again.

6.3.1 Clusters in the Base System

Referring to Chapter 5, clusters formed for original IEEE-39 bus test system (base-case) are shown in *Table 6.3*, *Figure 6.10 a*nd *Figure 6.11*.

Table 6.3: List of clusters for the base case

BASE CASE	
Cluster Number	**Buses Placed in Cluster**
1	28-29
2	12-32-37
3	31-35
4	20-33
5	36
6	38
7	21
8	2-3-4-5-6-7-8-10-11-13-14-15-16-17-18-24-25-26-27
9	1-9-19-22-23-30-39
10	34

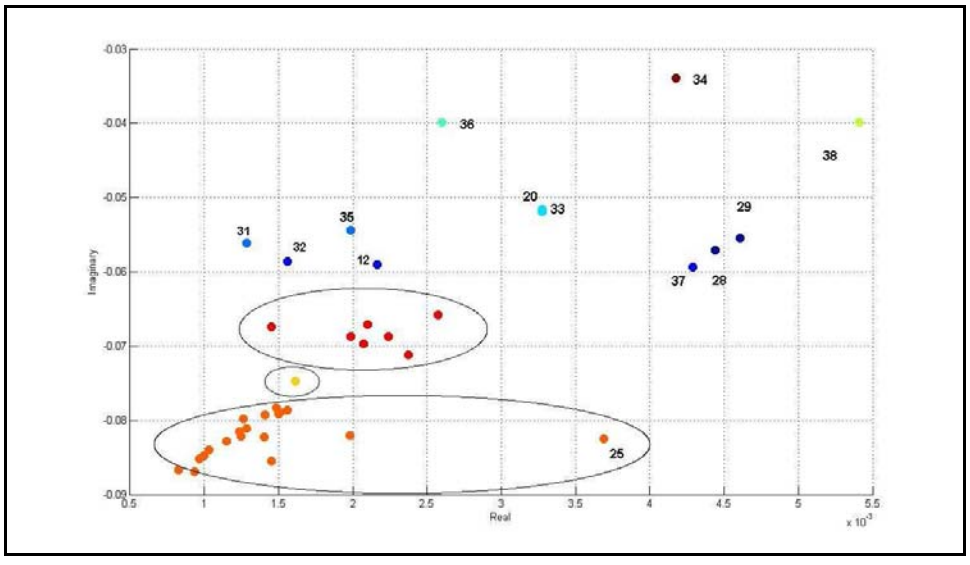

Figure 6.10: Clusters formed in IEEE 39 impedance matrix

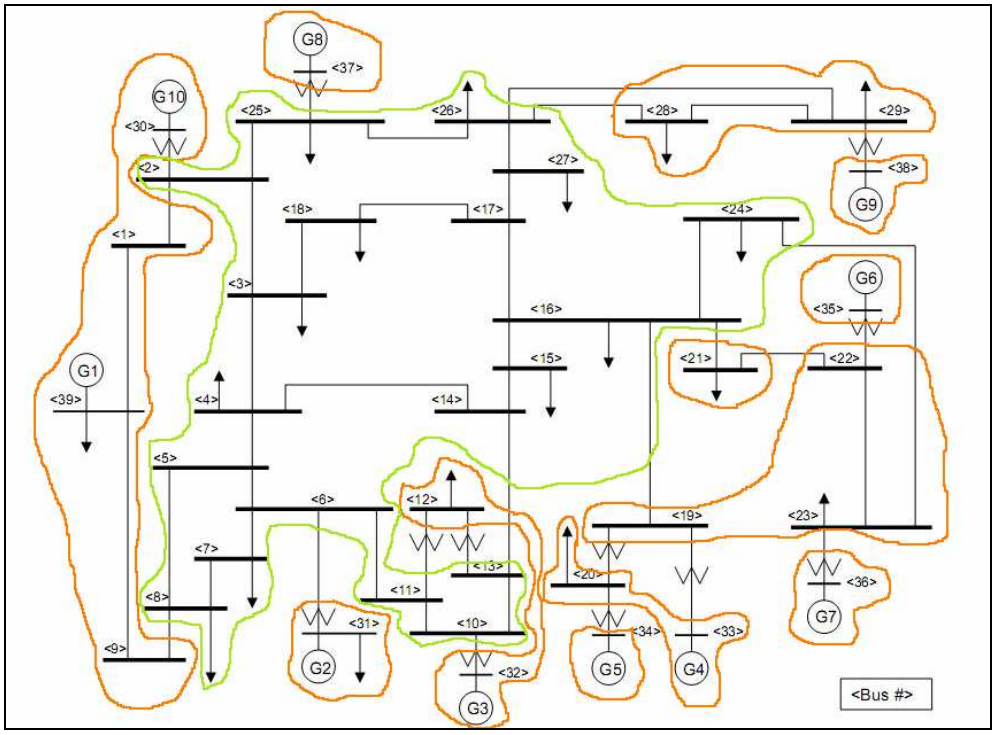

Figure 6.11: Grouping of the buses of IEEE 39 w.r.t. clustering of Z_{BUS}.

Case-C5

Simulation outputs contain impedance measurements taken at each end of the transmission lines. Majority of the lines are recorded but some of them are presented here for purposes of comparison. Case ID card describes details of the simulation. *Figure 6.13, 6.14* and *6.15* present outputs.

Table 6.4: Case ID Card for C5

Case ID	C-5
Fault Data	3-Phase Solid fault on Line 15-16
Fault initiated at (s) Fault period (s) Fault cleared at (s) Reclosure at (s)	0.1 0.1-0.45 0.45 No Reclosure
Lines observed	Line 2-1 (Line A) Line 9-39 (Line B) Line 8-9 (Line C) Line 8-5 (Line D) Line 17-16 (Line E) Line 1-39 (line F)

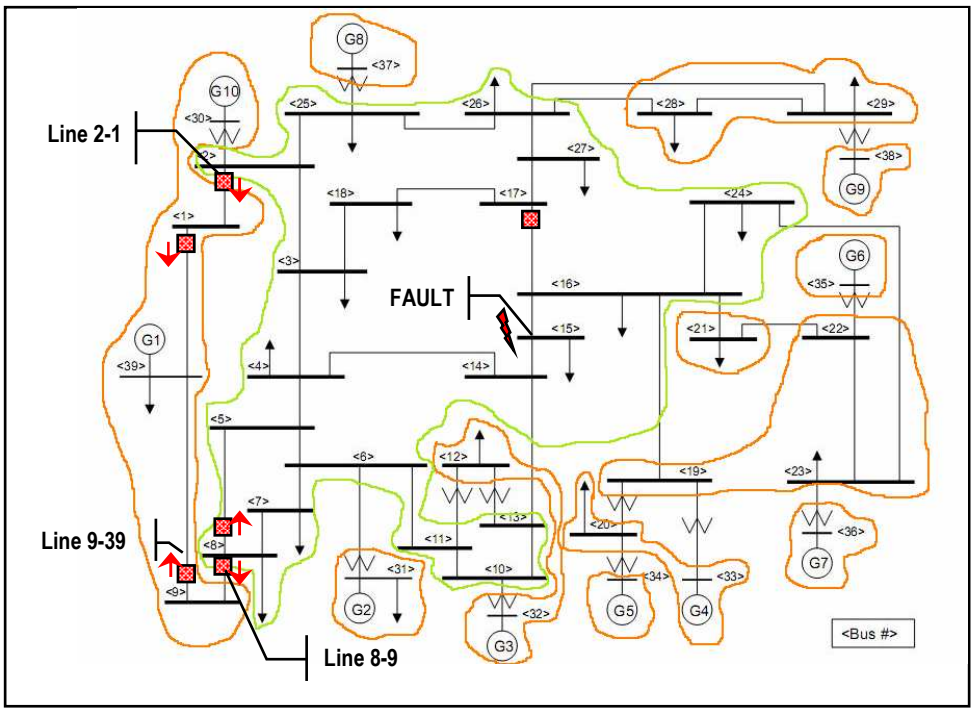

Figure 6.12: Case Layout for case C5

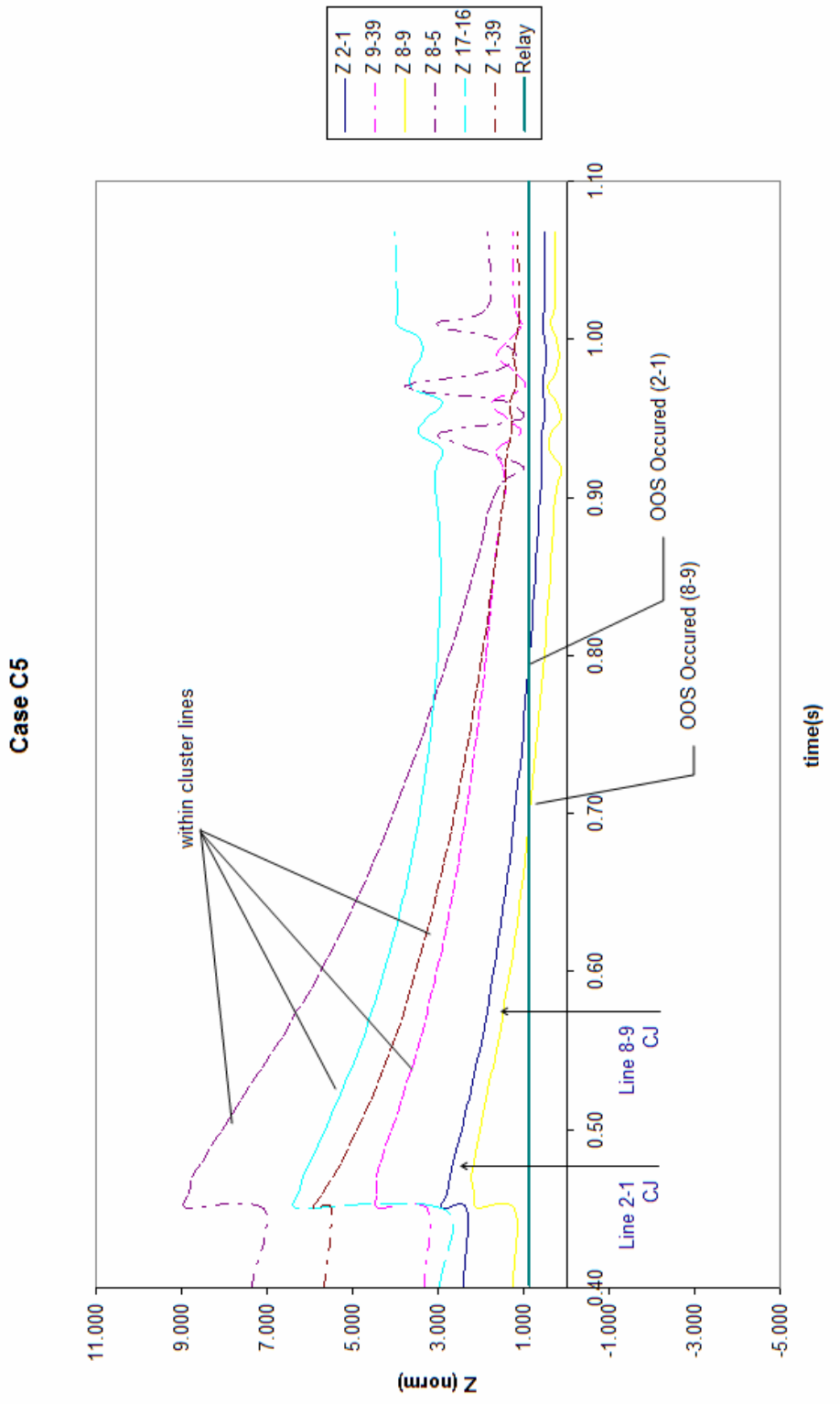

Figure 6.13: Line Impedance values and OOS order for case C5**.**

Dotted lines in *Figure 6.12* correspond to transmission links connecting buses placed in the same cluster. It is worth to give an example to be more clear. Line 9-39 (pink colored line) is connecting buses 9 and 39. Both of these buses are placed in Cluster #9 according to *Table 6.3*. This line is named as *"within cluster line"* (WC) as it connects buses placed in the same cluster. Conversely, line 2-1 connects buses 2 and 1 which are placed on different clusters. Line 2-1 is named as *"Cluster Joining"* (CJ) branch for that reason.

Among the lines shown in Figure 6.13, two CJ lines exist. (line 2-1 and 8-9). Also, these two lines are only lines facing OOS under the power impact of case C5. Remaining lines are all WC and also their swing locus passes above the 0.86 pu relay tripping region.

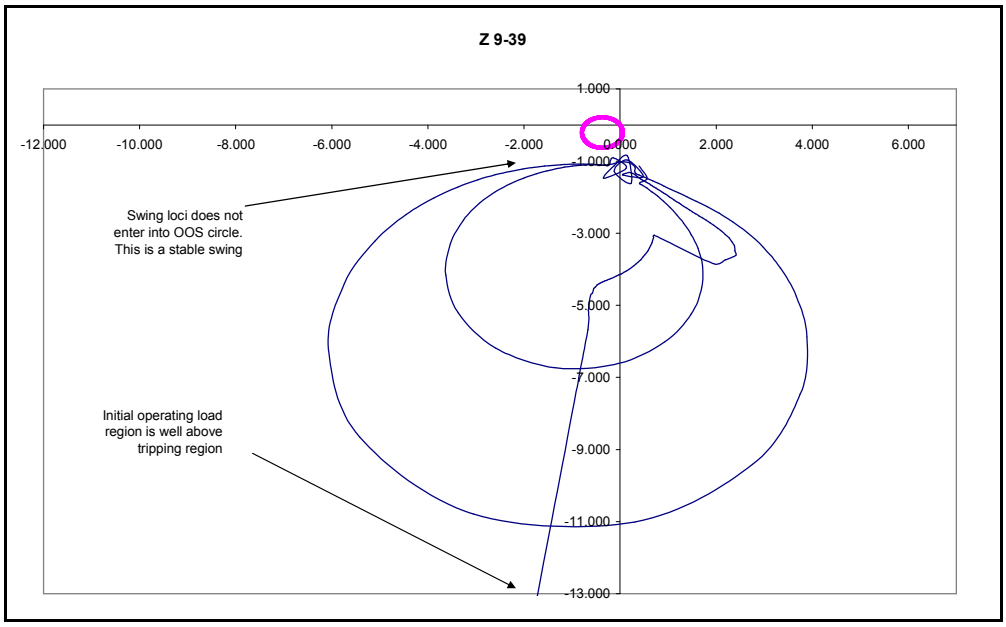

Figure 6.14: RX-diagram for line 9-39

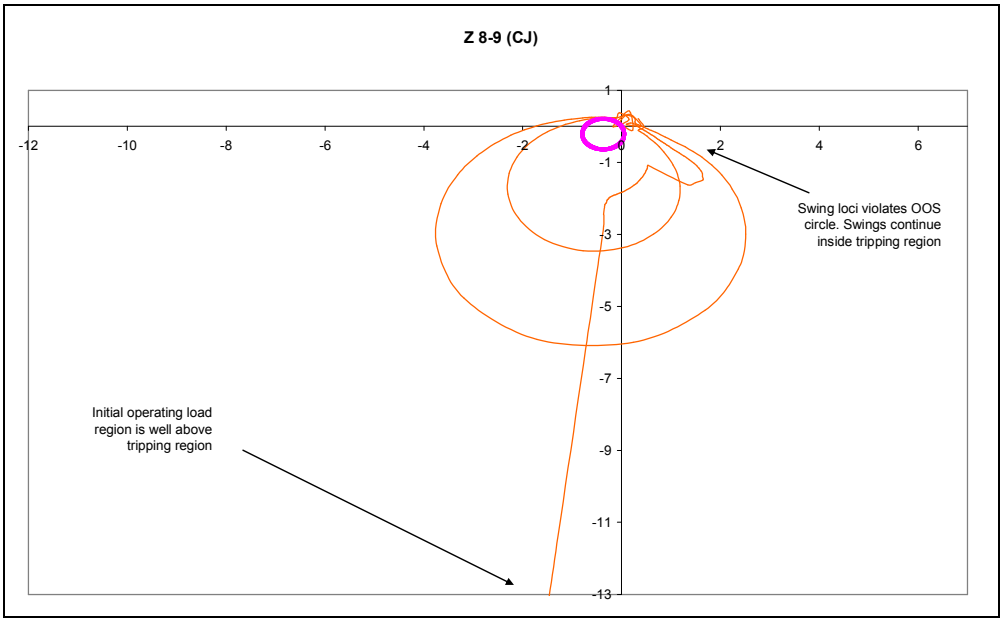

Figure 6.15: RX-diagram for line 8-9 which is Cluster-Joining branch.

R-X diagrams show the swing locus movements for two lines, first one in *Figure 6.14* is located within same cluster (9-39). Swing is moving close to the tripping region (pink circle), especially for the first overshoot period (larger circular path). However, swing locus has not crossed the tripping region and has found a new stable point.

Next R-X diagram in *Figure 6.15* belongs to a cluster-joining branch (8-9). Same type of movement is observed, but this time locus crosses the tripping circle. It is not really important that locus crosses the circle once. This tripping can be ignored by the use of a Power Swing Blocking (PSB) function. However, locus places on an operating point inside the tripping circle. This swing is not a stable swing and shows an Out-of-Step condition. Hence; cluster-joining branch is experiencing an OOS condition.

One can ask about the reverse characteristics of the R-X diagrams. Since power flow is negative on those branches, i.e. current is injected not out of but into the bus, negative impedances are observed on diagrams. Normally, distance relay OOS function is not active on reverse-polarity swings. Reverse swing is detected by the relay placed on the other end of the line. Impedance measurement on both ends of the line can be taken as equal if small active and reactive losses are neglected. Hence negative impedance on relay 8-9 is equivalent to positive impedance measured by relay 9-8. Line will be either WC or CJ not depending on which end is used as measurement terminal. Reverse polarity shown on R-X diagrams does not affect the theory tested here, rather it is just a matter of power flow direction.

Result of case C-5 shows that OOS condition is observed on CJs before WC branches. As mentioned earlier, investigation is not limited to 6 lines shown on *Figure 6.12 ,* but rather 16 lines are observed for OOS. Line 2-1 and Line 8-9 are entering OOS circle before the WC lines. Note that those buses are placed remote from the fault location. Namely, these two links are more vulnerable to face OOS than other lines of the network for the base topology.(base case of IEEE-39)

Type of behaviour observed in case C-5 can be stemmed from different power system parameters and may cause misunderstanding. A type of self-check is tried for that sense.

6.3.1 Clusters in the Modified System

Modified Case

Line 2-1 is a cluster-joining branch connecting two separate clusters for the base case. In order to change cluster formation, line 2-1 is modified by adding a parallel line with R=0.00100, X= 0.01110, B= 0.23870, (i.e., impedance between buses 2 and 1 is reduced to ¼ of the original line). It is aimed to reduce impedance between buses 2 and 1. Line parameters are chosen so that buses 2 and 1 will be placed on the same cluster.

As network topology is modified, so does bus impedance matrix. Data clustering algorithm is applied to the modified network and new clusters are formed as summarized in *Table 6.5* and in *Figure 6.16*.

Table 6.5: Clusters in the modified system

MODIFIED CASE	
Cluster Number	**Buses Included**
1	31
2	32-12
3	20-28-29-33-35
4	37
5	1-9-21
6	2-3-4-5-6-7-8-10-11-13-14-15-16-17-18-24-25-26-27-39
7	36
8	38
9	34
10	19-22-23-30

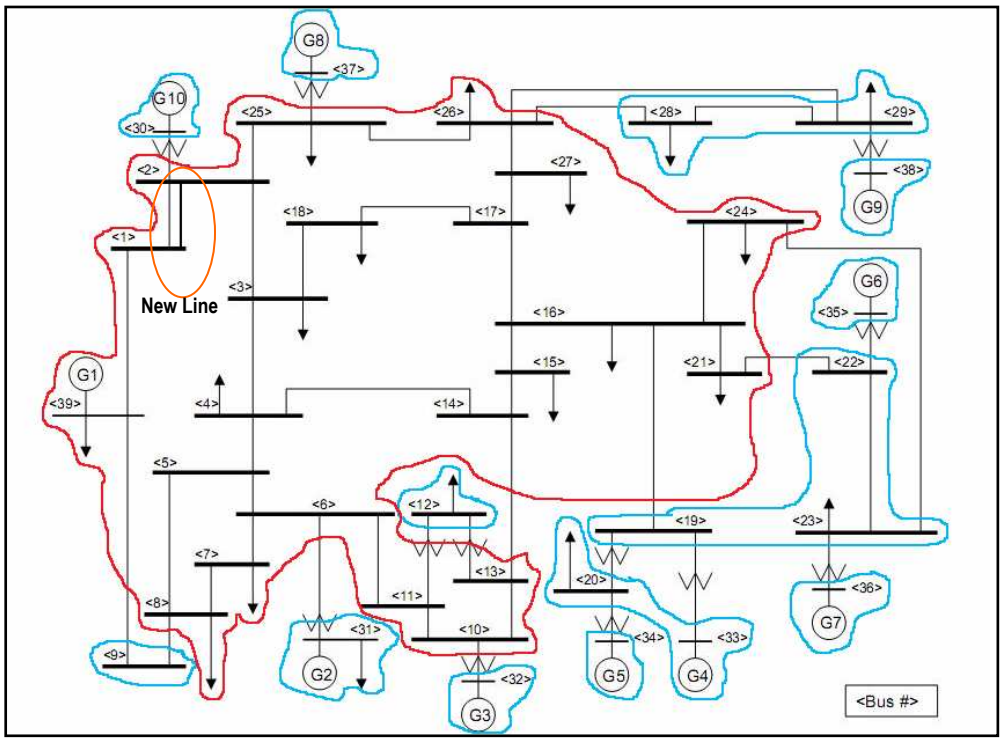

Figure 6.16: Grouping the buses of modified IEEE-39 w.r.t. clustering of Z_{BUS}

Bus 2 is integrated into the biggest cluster as aimed at the beginning. Note that buses 1, 9 and 39 are not placed in the same cluster anymore. Hence, Line 2-1 is not WC line anymore. Line 9-39 becomes CJ as it joins buses in two separate clusters.

Case C6

Same fault of case C5 is applied to the modified test system.

Table 6.6: Case ID card for C6.

Case ID	C-5
Fault Data	3-Phase Solid fault on Line 15-16
Fault initiated at (s) Fault period (s) Fault cleared at (s) Reclosure at (s)	0.1 0.1-0.45 0.45 No Reclosure
Lines observed	Line 2-1 Line 9-39 Line 8-9 Line 8-5 Line 17-16 Line 1-39

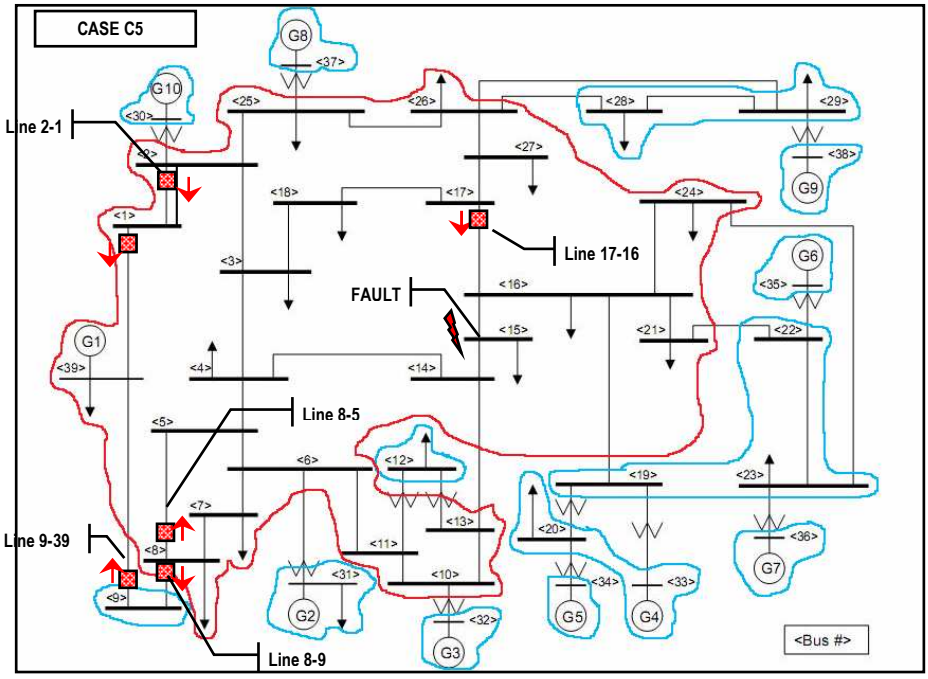

Figure 6.17: Case Layout for C6

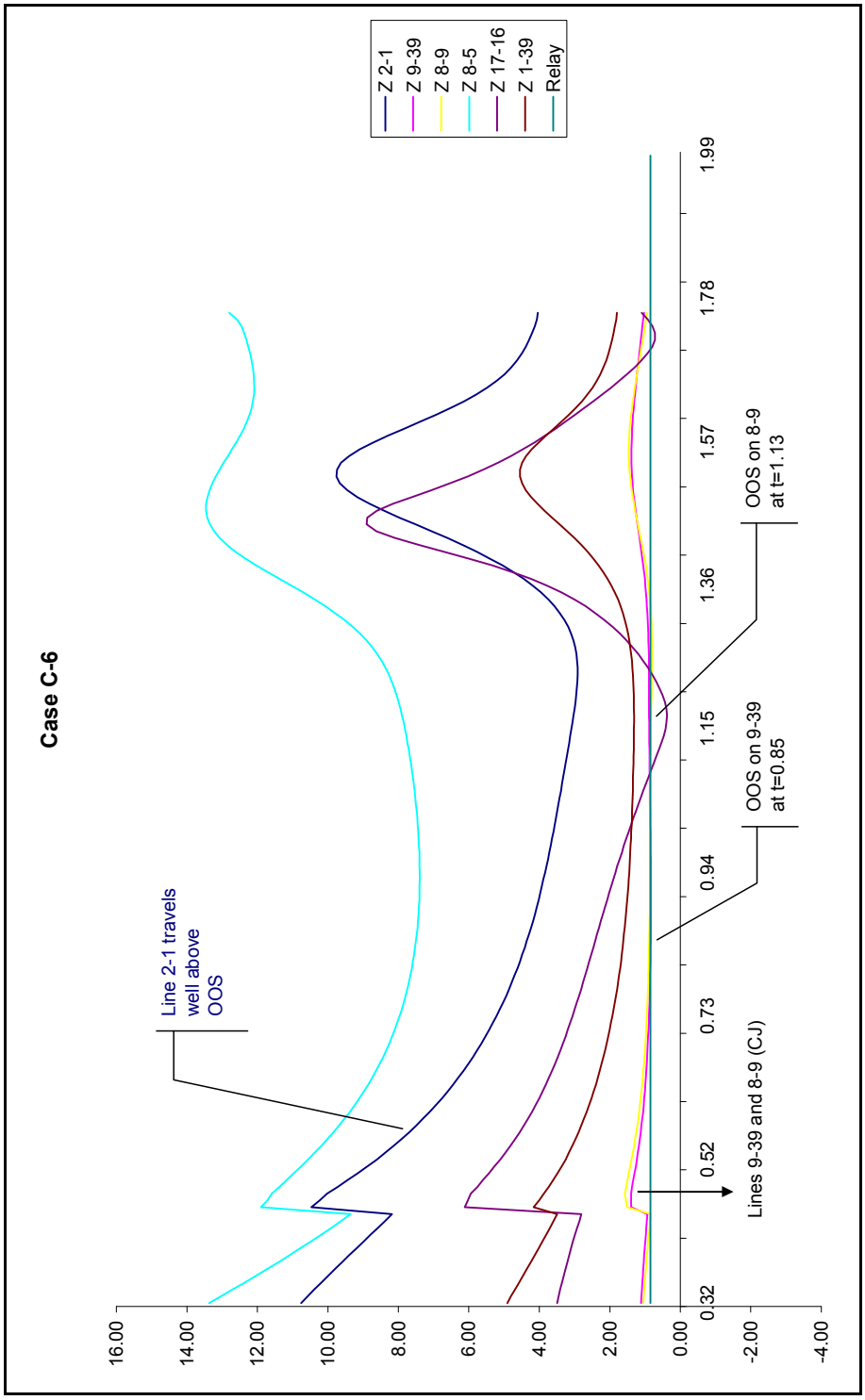

Figure 6.18: Line Impedance values and OOS order for case C6.

There are major differences on swing behaviours of lines 2-1 and 9-39 as compared to original network topology. Line 2-1 has shifted from CJ to WC after modification. Impedance locus for line 2-1 is now well above OOS point whereas it was crossing OOS point at t=0.81 for the base topology.

Line 9-39 was placed as a WC line and not experiencing OOS in the base case. For the modified topology, line 9-39 moved to CJ and has faced OOS at t=0.85 which is 2nd earliest OOS among investigated lines.

Line 17-16 for case C6 is facing a rapid OOS although not expected by cluster analysis. This line is very close to fault location (line15-16) and it would be possible to reach OOS for lines close to the fault point since power impacts will be larger for closer points.

Comparison graphs and R-X diagrams for lines 2-1, 9-39 and 8-9 are given. *(Figure 6.19 to 6.24)*

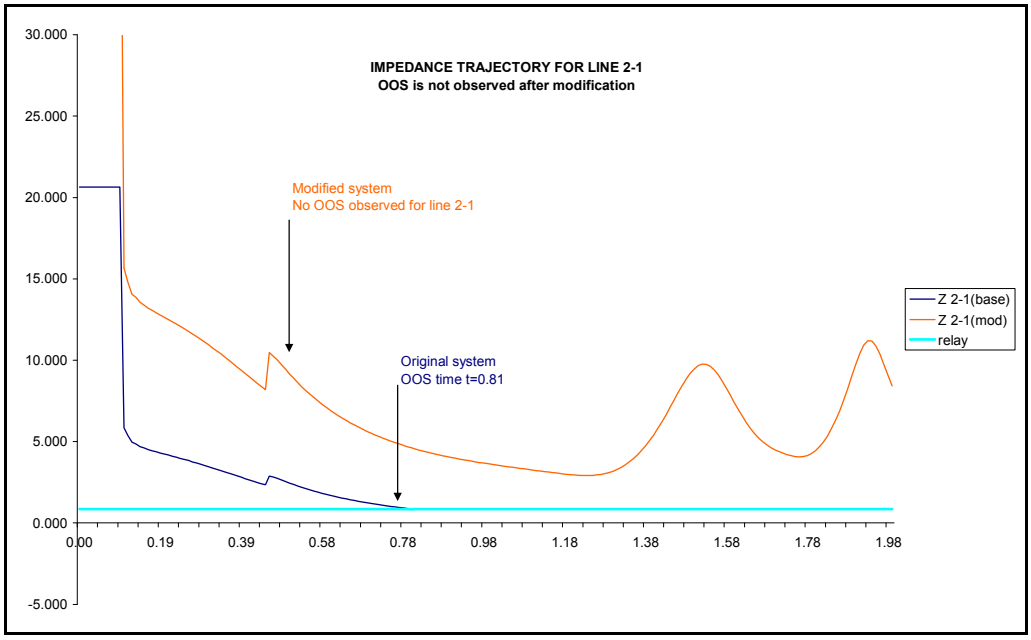

Figure 6.19: Comparison of line impedance for line 2-1 between original and modified systems.

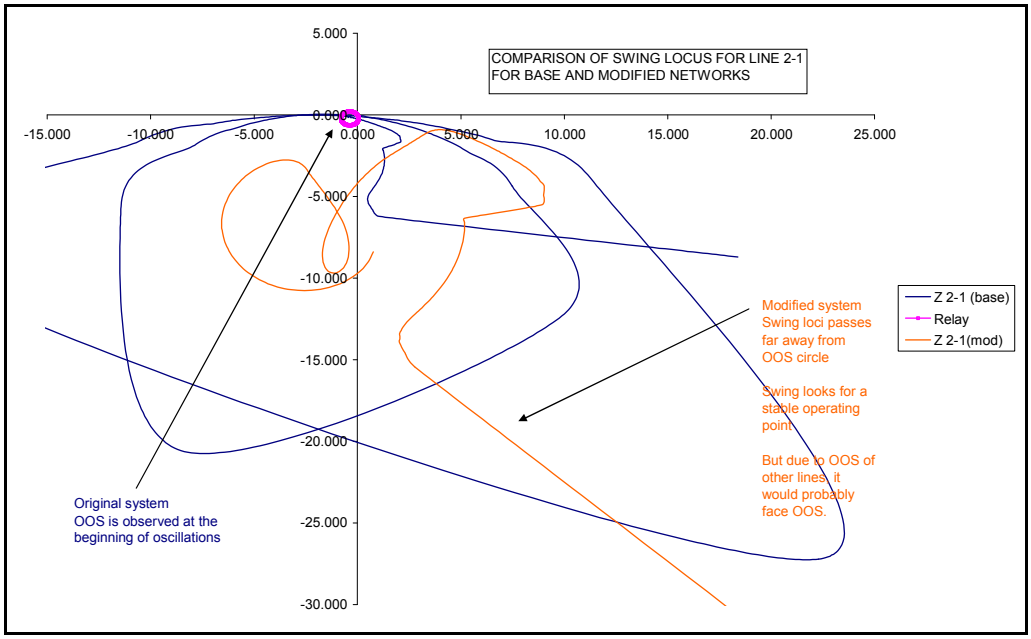

Figure 6.20: Comparison of R-X plane swing loci movements of line 2-1 with base and modified network topologies.

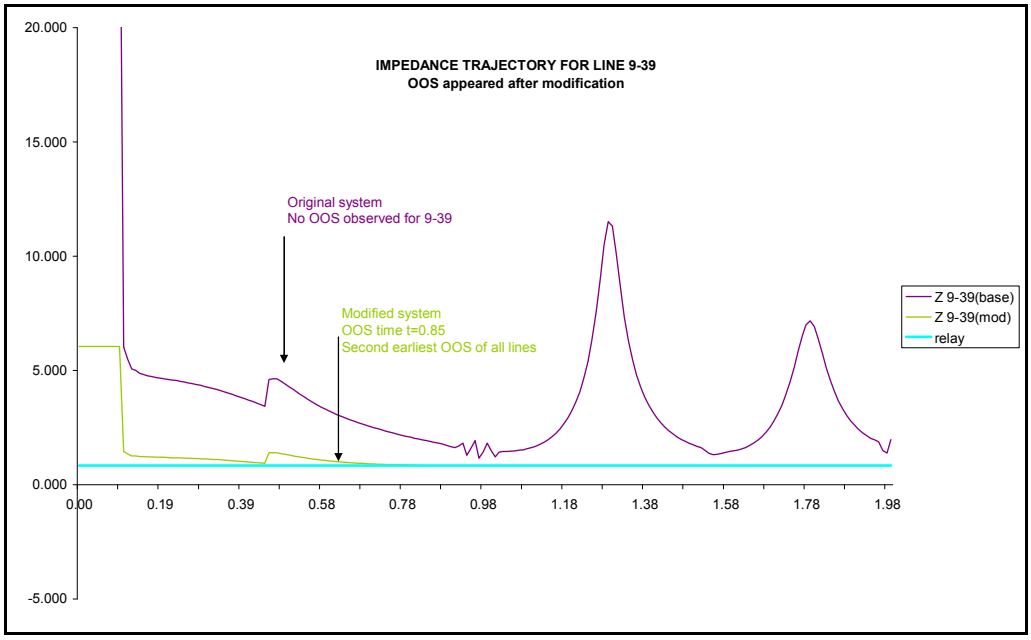

Figure 6.21: Comparison of line impedance for line 9-39 between original and modified systems.

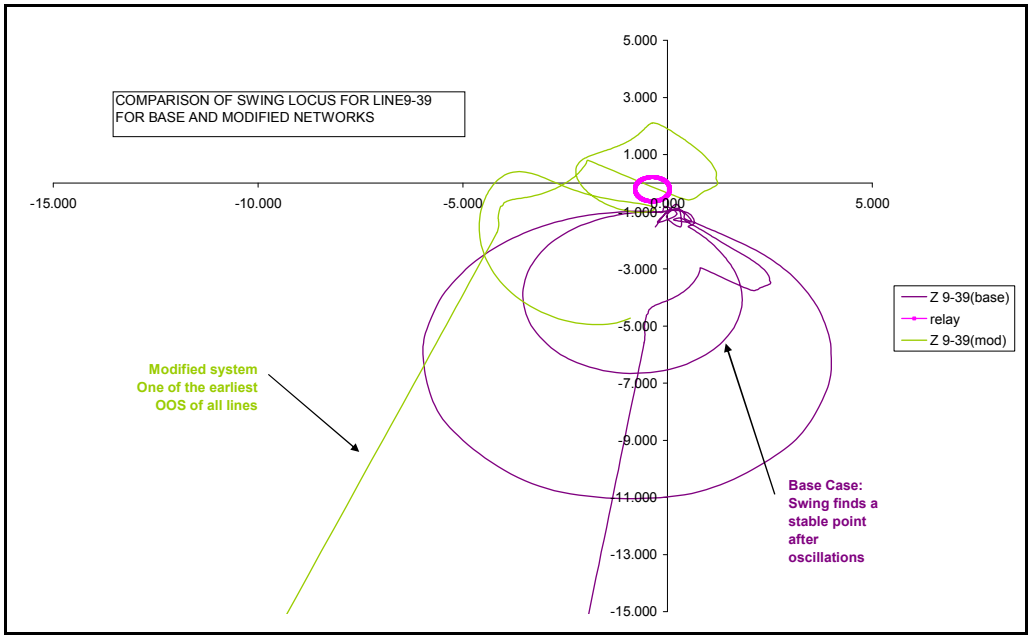

Figure 6.22: Comparison of R-X plane swing loci movements of line 9-39 on base and modified network topologies.

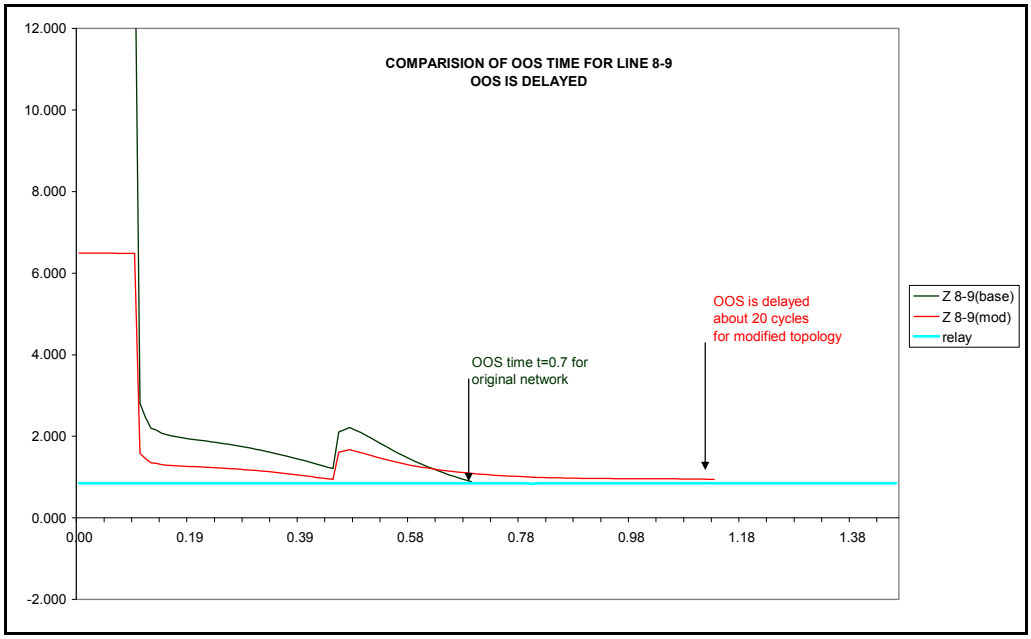

Figure 6.23: Comparison of line impedance for line 8-9 between original and modified systems.

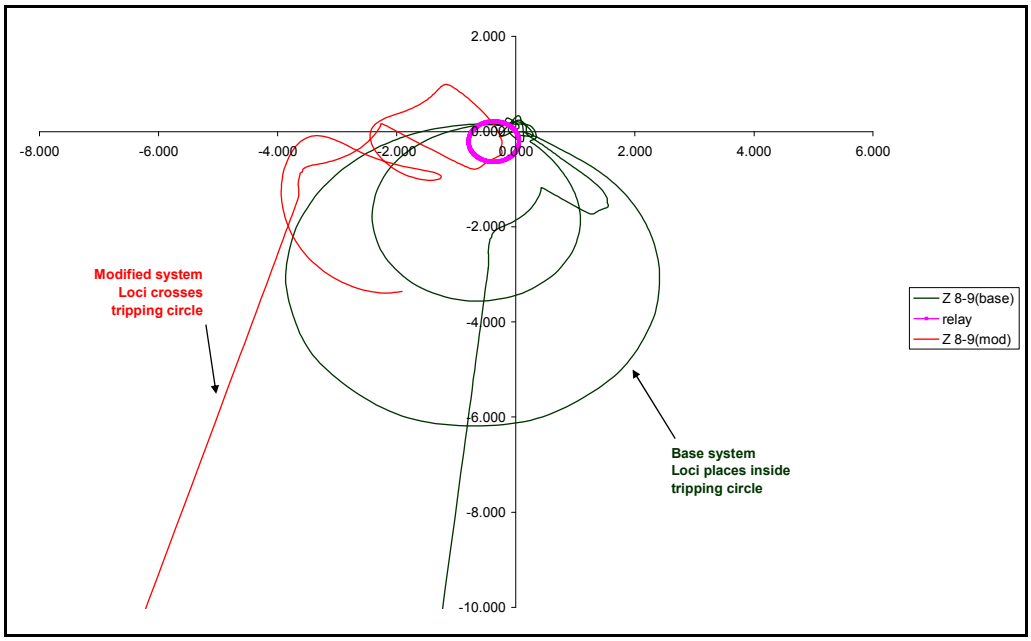

Figure 6.24: Comparison of R-X plane swing loci movements of line 8-9 on base and modified network topologies.

6.5 COPHENET VALUE AS A MEASURE OF SYSTEM STABILITY

In statistics, cophenet value is used as a measure for the success of the clustering the data group. It has a range of 0 to 1 and clustering algorithm is referred as successful, if cophenet is close to 1. Successful clustered data group has data points widely separated from each other; no data places on the same distance to other data point. If all data in the group are identical, then clustering becomes impossible leading to cophenet value of zero.

As power system has stronger transmission links, short circuit ratings of the buses becomes closer to each other. Because; as alternative paths are created for power flow, equivalent line impedance in-between neighbor buses decreases.

As alternative load flow paths are installed on an existing system, clustering of the Z bus becomes harder, leading to a lower cophenet value. It can be concluded that, more OOS vulnerable the system is, it is easier to cluster buses and is higher the cophenet value.

IEEE 39 bus system is modified by adding new line in chapter 6. Modified system is shown to be more stable than the original one. Additionally, some other modifications are tried on IEEE 39 bus system. Cophenet values for these data groups are given in *Table 6.7*.

Table 6.7: Cophenet values for modified IEEE 39 network configurations

Case	Cophenet value
IEEE 39 - base case	0.8539
New line installed between buses 2 and 1	0.8292
New line installed between buses 4 and 39	0.8383
New line installed between buses 8 and 39	0.8089

As new lines are added to existing configuration, cophenet value decreases meaning that it becomes more difficult to cluster buses. Buses are forced to be

collected within one global cluster as bus impedances are approaching to each other by the addition of new lines. Transmission bottlenecks are decreased in number, leading to a more stable system with lower cophenet value.

By using the cophenet value for different configurations, power system planner can decide which part of the power system needs additional lines by only considering stability point of view. Among the modifications in Table 6.7, adding a new line between buses 8 and 39 is more appropriate than other modifications to improve stability of the test system.

CHAPTER 7

TEST ON TURKISH POWER SYSTEM

7.1 GENERAL

Turkish Transmission System is a large interconnected system with three different voltage levels, i.e. 66 kV, 154 kV and 380 kV.

Clustering method introduced in this study, is applied to 380 kV buses of the Turkish Transmission system. Short-circuit ratings of the buses are reported annually by Turkish Transmission System Operator (TEIAS). Data in this study is taken from the work of 2007 regarding summer peak load of 26.07.2007 at 11:00 a.m.

Number of 380 kV buses is 79 on the date of 2007. It would be higher when 2009 is considered. Also, one should be aware that, short-circuit rating (in kA) of these buses may have been improved by the connection of new feeders to the existing system.

It is aimed to show that the method is not only useful for a future system. It is also easily applicable to an existing system.

A practical advantage of the method is worth to mention here. Clustering method does not dependent on the unit of Z entities. It is just a matter of

comparison, hence; either ohms or p.u. can be used for the purpose of distance measurement on R-X plane. Ohm values are used for Turkish System, whereas, p.u values have been employed for IEEE 39 bus test system in Chapter 7.

Scattering of Z values on R-X plane are shown in *Figure 7.1*.

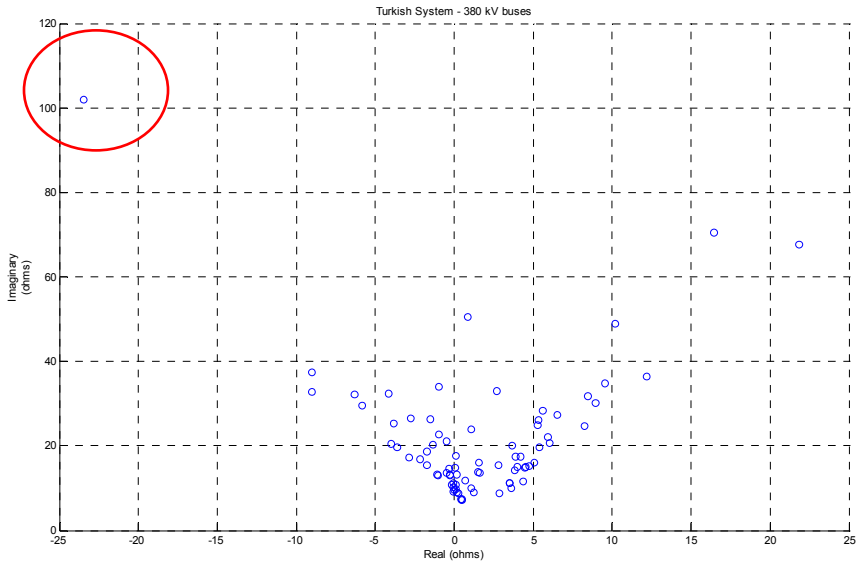

Figure 7.1: Scattering of 380 kV TEIAS buses on R-X plane.

7.2 PRE-MODIFICATION OF 2007 DATA GROUP

There exists a bus on the left-most of the R-X axis. It is seen to be wide-apart from all the remaining buses. Deeper investigation on the data group revealed that this bus is Davutpasa 380 kV bus. Its behavior does not seem to be a realistic one since Davutpasa is on the middle of Istanbul region and must have a closer short-circuit capacity with its neighbor buses (i.e. Ikitelli 380kV, Ikitelli 154 kV and Davutpasa 154 kV buses).

Comparison of SC ratings presented in 2007 and 2008 data of Davutpasa and Ikitelli (both 154 and 380 kV) buses are given in *Table 7.1*.

Table 7.1: Short circuit values for Davutpasa and Ikitelli.

	3 phase SC current(kA)		
Bus Name	**2007 data**	**2008 data**	**K**
Davutpasa 380	2.1*	19.7	9.38
Davutpasa 154	15.6	24.6	1.58
Ikitelli 380	19.5	24.7	1.27
Ikitelli 154	15.6	24.6	1.58

Improvement constant K is the ratio of 2008 values to 2007 values. Davutpasa 380 kV bus experienced an unpredictable improvement between 2007 and 2008 although 154 kV side is well on the limit and similar for Ikitelli 380 kV and Ikitelli 154 kV buses.

There seems a problem with the current value of Davutpasa 380 kV bus in data group 2007, hence; it is better to modify data of Davutpasa bus. 2007 TEIAS data is modified with Davutpasa bus projected SC rating of 15.5 kA. Improvement constant K=1.27 is taken as it is equal to K of Ikitelli 380 kV bus.

Modified data is again scattered on R-X plane. (*Figure 7.2*)

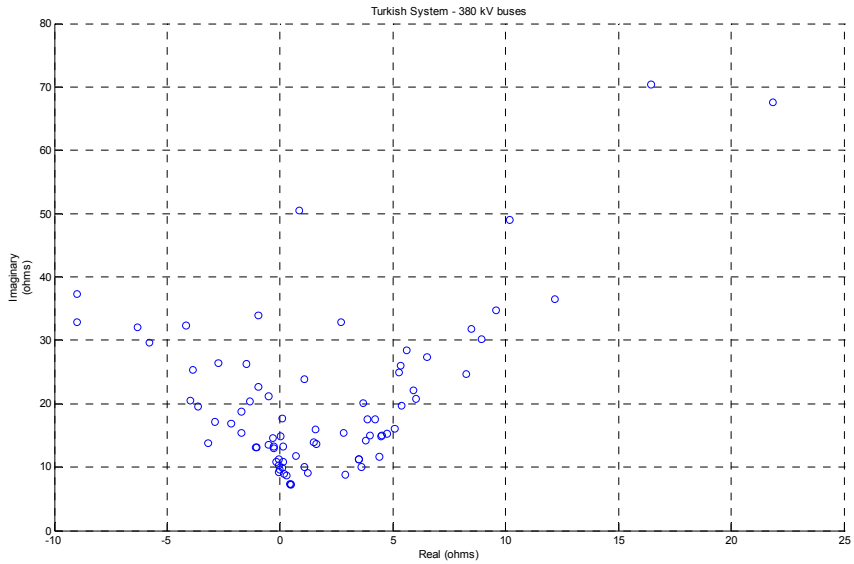

Figure 7.2: Scattering of 380 kV TEIAS buses on R-X plane.(modified)

7.3 CLUSTERING OF TURKISH SYSTEM

Clustering algorithm is applied on the Turkish data. Distance matrix of size 79x79 is formed. Scatters of the clustering steps are shown.

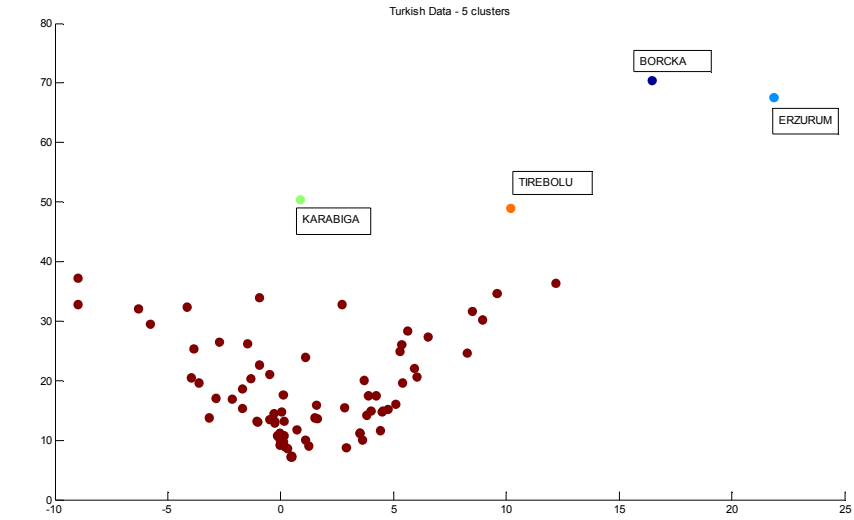

Figure 7.3: Turkish EPS 5 clusters formed

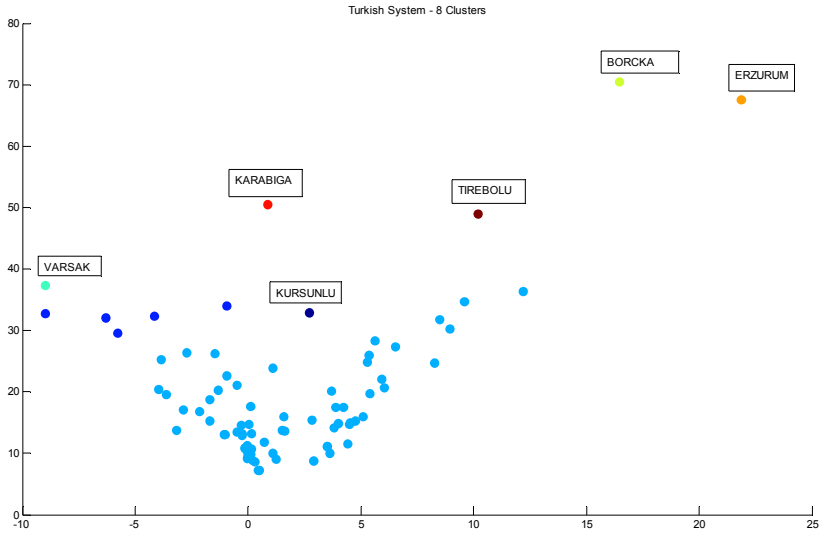

Figure 7.4: Turkish EPS 8 clusters formed

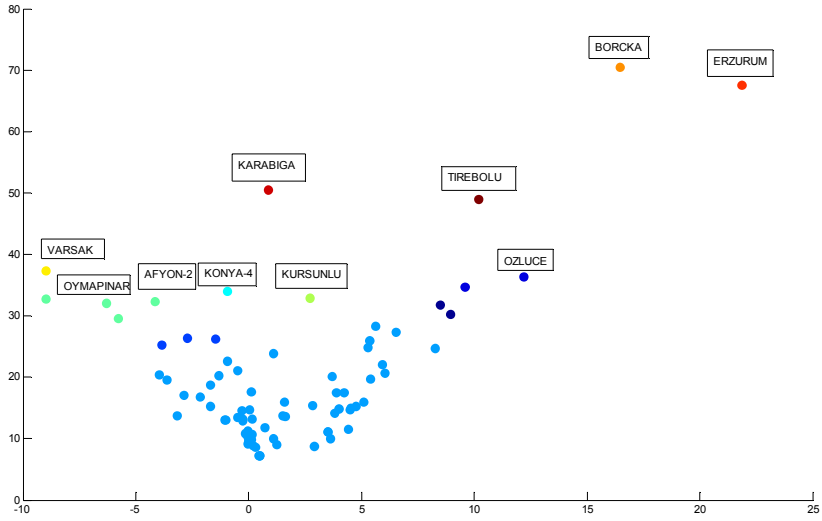

Figure 7.5: Turkish EPS 12 clusters formed

In statistics, cophenet value is a measure of how separate are the elements of different clusters. Clustering is regarded as successful if cophenet is close to one.

Cophenet value, which defines the success of the clustering algorithm, is found as 0.893 for the clustering of Turkish 380 kV system. Turkish 380 kV network seems to be a stable one by considering this lower cophenet value. Namely, Turkish system can not be clustered easily, which means it is also difficult to face OOS condition on the transmission lines.

Borcka and Tirebolu buses are comparably separated from rest of the system. Line connecting Borcka and Tirebolu buses can be regarded as a weak link. It is one of the expected lines to face OOS, if enough power impact is experienced by faults or switching operations.

CHAPTER 8

CONCLUSION

8.1 GENERAL

Interconnected power systems promise operational benefits like reserve capacity, reliability, stable voltage and frequency. Economic benefits like optimization in the use of reserve capacities and smoothing daily-load curve are also valid.

However, power systems will be more vulnerable to power impacts as they improve both in length and capacity. Dynamic properties of a large power network are dependant on several implicitly connected parameters which is hard to determine correctly. Amount of data need to be collected and verified is also a burden to the analyzer, especially for the power system planner, as transmission network gets larger.

Starting from 2002, Turkish Electrical System is planned to be synchronously connected to the European grid, namely UCTE. Turkish Electrical System is a large interconnected system by itself with 42,000 MW installed capacity. Synchronous connection requirements of former UCTE (now ETSO-E) need careful analysis of system configurations in different network scenarios but dynamic analysis is a challenging and computationally difficult task for the analyzer as the number of buses increases.

Some transmission links in a given power network may be termed as bottle-necks restricting power flows in case of a power impact. It is often necessary to determine or at least estimate weak transmission links on network planning step. Theory of the thesis is stemmed from the fact that amount of available data is very limited and hard to reach and validate as it is experienced during practices on Turkey-UCTE connection task studies. Hence, a more practical approach is needed in order to guess weak transmission links without performing detailed dynamic simulations.

Method will be beneficial to the power system planner as he decides new improvements on current network topology and has to foresee possible adverse-effects on system stability.

8.2 DISCUSSION

Out-of-Step phenomenon is used to determine the weakness of the line. Out-of-Step is expected to be seen on rather longer lines with larger line impedance. Theory of the thesis is based on the fact that long transmission lines connect buses with considerably different short-circuit impedances. If one bus has closer short circuit capacity to its neighbor bus, in-between impedance (i.e. line impedance) of these lines will be fairly small. Taking the case to minimum limit, if a theoretical zero impedance line is inserted between two buses, they will, electrically, be identical buses with equal short circuit ratings. Buses with close short-circuit capacity are grouped in the same cluster when placed on the euclidean space. Shorter lines are hardly expected to face OOS as compared to longer lines.

If a long line is inserted between two lines, they become fairly distant to each other in euclidean space. Taking the case to infinite limit; if an existing line is broken between two buses, which is equivalent to infinite impedance or infinite line length, short-circuit ratings of these buses will move away from each other. They will place in separate clusters, hence; OOS will be expected on that

line.

Out-of-Step phenomenon is presented in the literature with two important properties [28]. **For a given network** and **loading conditions**, OOS is observed in a definite sequence and in some pre-determined weak links of the system. Sequence is not dependant on the initial fault location and fault severity. These two *"conjectures"* are verified with cases C1 to C4.

Defining weak links of the system is the main scope of this thesis. A severe fault is applied to the base test system in case C5 and OOS sequence is observed to be consistent with the clusters defined in chapter 5. System is modified by adding a new line between buses. New clusters are defined since network topology and hence impedance matrix is modified, too. OOS sequence is not the same as the one in base-case but is still consistent with the clusters re-calculated. Change of sequence is consistent with the OOS theory presented in [28] since *"conjecture*" is valid only for a given network topology.

Cophenet value found among the cluster groupings is suggested to be an indice defining overall stability level of the power system.

Clustering method is also applied on the Turkish 380 kV system and shown to be easily applicable to a large electrical system.

8.3 FUTURE WORK

Simulation results reveal a fact that, although method is very successful for beforehand determination of possible weak links of the system; clustering is not fully capable of defining all OOS links but still valid to determine possible points. Lines placed close to the fault location (as one in case C6) may face OOS since power impacts will be larger on these points. However, this will not disturb the generally-applicable property of the main theory.

In addition to the validity for a given network configuration*, conjecture* of OOS also dictates another restriction as it is valid for a given "loading condition". Impedance matrix does not contain information on the current loading levels of transmission lines, hence; future work on the theory may use another power system variable instead of impedance matrix taking into account both "network configuration" and "loading condition" as *conjecture* states.

REFERENCES

[1] Rüdenberg, R. (1950). *Transient Performance of Electric Power Systems; Phenomena in Lumped Networks.*, New York: McGraw-Hill.

[2] "Power Swing and Out-of-Step Considerations on Transmission Lines", (2005), IEEE Power System Relaying Committee Report, RC WG D6.

[3] Mason, C.R., (1956), *The Art and Science of Protective Relaying,* General Electric.

[4] Kaufmann, M. (eds.) (1997). *Power System Protection Volume-I: Principles and Components*, London: The Institution of Electrical Engineers.

[5] Ziegler, G. (1999). *Numerical Distance Protection*, Erlangen: Publicis Corporate Publishing- Siemens.

[6] Reimert, D., (2006), *Protective Relaying for Power Generation Systems*, Boca Raton, FL: CRC Press.

[7] Mooney, J., Fischer, N., (2005), "Application Guidelines for Power Swing Detection on Transmission Lines", Schweitzer Engineering Laboratories, USA.

[8] Berdy, J., "Application of Out-of-Step Blocking and Tripping Relays", General Electric.

[9] Peterson, W.L., Makram, E.B., and Baldwin, T.L., (1989), "A Generalized PC-based Bus Impedance Matrix Building Algorithm", *IEEE Energy and Information Technologies Conf. in the Southeast*, **2**, pp. 432–436.

[10] Yang, X.P., et al., (2007), "Novel Applications of Z-matrix to Network Topology Analysis in the Relay Coordination Software", *IET Generation Transmission Distribution*, 1(4), pp. 540-547.

[11] Brown, H.E., (1967), "Short Circuit Studies of Large Systems by the Impedance Matrix Method", *Proceedings of IEEE PICA Conf*erence, Pittsburgh, PA, pp. 335–342.

[12] Qin, B.-L., and Guzman-Casillas, A., (2000), "A New Method for Protection Zone Selection in Microprocessor-based Bus Relay*"*", *IEEE Transactions on Power Delivery*, **10**(1), pp. 876–887.

[13] Makram, E.B., Thorton, K.P., and Brown, H.E., (1989), "Selection of Lines to be Switched to Eliminate Overloaded Lines Using a Z-matrix Method*"*, *IEEE Transactions on Power Systems*, 4(2), pp. 653–661.

[14] Jain, A.K., Murty, M.N., and Flynn, P.J., (1999), "Data Clustering and its Applications", *ACM Computing Surveys*, **31**(3), pp. 264–323.

[15] Bills, G.W., et. al.,(1970), "On-line Stability Analysis Study", Report for the Edison Electric Institute, RP90-1.

[16] Athay, T, Podmor, R., and Virmani, S.,(1979), "A Practical Method for Direct Analysis of Transient Stability*"*, *IEEE Transactions on Power Apparatus and Systems*, **9(**2), pp. 573–584.

[17] Power Systems Test Case Archive, Last Visited on December 19, 2008, Web site: *http://www.ee.washington.edu/research/pstca/*

[18] Homepage of Dr. Pablo Ledesma, Last visited on November 5, 2008, Web Site: http://electrica.uc3m.es/pablole/varios_e.html

[19] "Isolation and Restoration Policies against System Collapse",(2002), CIGRE Publication Number: 200, WG34.08.

[20] Vassena et al., (2003), "A Probabilistic Approach to Power Systems Network Planning under Uncertainties", *IEEE Bologna Power Tech Conference*,Italy.

[21] Abdel-Galil, T., K., (2004), "Power Quality Disturbance Classification using the Inductive Inference Approach", *IEEE Transactions on Power Delivery*, Issue: 99, pp. 1-7.

[22] Kermanshahi, B., and Iwamiya, H., (2002), "Up to year 2020 Load Forecasting using Neural Nets", *International Journal of Electrical Power Energy Systems,* **24**(9), pp. 789-797.

[23] Zeynelgil, H. L., Demiroren, N. and Sengor, N.S., (2002), "The Application of ANN Technique to Automatic Generation Control for multi-area Power System", *International Journal of Electrical Power Energy Systems*, **24**(5), pp. 345-354.

[24] Vishwakarma,D. N., and Moravej, Z., (2001) "ANN-based directional overcurrent relay", *IEEE/PES Transmission and Distribution Conference and Exhibition (Cast No. 01CH37294),***1** , pp. 59-64.

[25] Tsanakas, A.D., Papaefthimiou,G. I., and Agoris, D.P., (2002), "Pollution Flashover Fault Analysis and Forecasting using Neural Networks", CIGRE Working Group 15.105.

[26] CIGRE, WG D1.11, (2006), "Data Mining Techniques and Applications in the Power Transmission Field", Publication Number: 292, Task Force 04.

[27] Mendelshon, N.S., (1956), “Some Elementary Properties of Ill Conditioned Matrices and Linear Equations*”. The American Mathematical Monthly,* **63**(5), pp. 285-295.

[28] Adibi, M.M., Kafka, R.J., and, Maram, S., (2006), “On Power System Controlled Separation”, *IEEE Transactions on Power Systems*, , 21(4), pp. 1894–1902.

APPENDIX

DIAGONALS OF BUS IMPEDANCE MATRIX

BASE CASE

DIAG =

(1,1)	0.0024 - 0.0712i
(2,1)	0.0015 - 0.0856i
(3,1)	0.0009 - 0.0869i
(4,1)	0.0010 - 0.0840i
(5,1)	0.0012 - 0.0816i
(6,1)	0.0013 - 0.0811i
(7,1)	0.0015 - 0.0783i
(8,1)	0.0014 - 0.0792i
(9,1)	0.0021 - 0.0697i
(10,1)	0.0016 - 0.0786i
(11,1)	0.0015 - 0.0790i
(12,1)	0.0022 - 0.0590i
(13,1)	0.0015 - 0.0792i
(14,1)	0.0012 - 0.0828i
(15,1)	0.0012 - 0.0822i
(16,1)	0.0010 - 0.0848i
(17,1)	0.0008 - 0.0868i
(18,1)	0.0010 - 0.0852i
(19,1)	0.0026 - 0.0658i
(20,1)	0.0033 - 0.0520i
(21,1)	0.0016 - 0.0748i
(22,1)	0.0020 - 0.0687i
(23,1)	0.0021 - 0.0671i
(24,1)	0.0013 - 0.0798i
(25,1)	0.0037 - 0.0825i
(26,1)	0.0020 - 0.0821i
(27,1)	0.0014 - 0.0823i
(28,1)	0.0044 - 0.0571i
(29,1)	0.0046 - 0.0555i
(30,1)	0.0015 - 0.0675i
(31,1)	0.0013 - 0.0561i
(32,1)	0.0016 - 0.0586i
(33,1)	0.0033 - 0.0516i
(34,1)	0.0042 - 0.0340i
(35,1)	0.0020 - 0.0544i
(36,1)	0.0026 - 0.0399i
(37,1)	0.0043 - 0.0593i
(38,1)	0.0054 - 0.0399i
(39,1)	0.0022 - 0.0687i

DIAGONALS OF BUS IMPEDANCE MATRIX

LINE REDUCED BETWEEN BUSES 2 AND 1
(MODIFIED CASE)

DIAG =

(1,1)	0.0015 - 0.0819i
(2,1)	0.0012 - 0.0855i
(3,1)	0.0008 - 0.0857i
(4,1)	0.0010 - 0.0819i
(5,1)	0.0012 - 0.0793i
(6,1)	0.0013 - 0.0789i
(7,1)	0.0015 - 0.0761i
(8,1)	0.0014 - 0.0771i
(9,1)	0.0018 - 0.0704i
(10,1)	0.0016 - 0.0764i
(11,1)	0.0015 - 0.0767i
(12,1)	0.0022 - 0.0568i
(13,1)	0.0015 - 0.0770i
(14,1)	0.0011 - 0.0806i
(15,1)	0.0012 - 0.0802i
(16,1)	0.0010 - 0.0830i
(17,1)	0.0008 - 0.0852i
(18,1)	0.0009 - 0.0838i
(19,1)	0.0025 - 0.0640i
(20,1)	0.0032 - 0.0502i
(21,1)	0.0016 - 0.0730i
(22,1)	0.0020 - 0.0669i
(23,1)	0.0021 - 0.0653i
(24,1)	0.0012 - 0.0780i
(25,1)	0.0036 - 0.0823i
(26,1)	0.0019 - 0.0811i
(27,1)	0.0014 - 0.0810i
(28,1)	0.0044 - 0.0560i
(29,1)	0.0046 - 0.0544i
(30,1)	0.0012 - 0.0674i
(31,1)	0.0013 - 0.0539i
(32,1)	0.0016 - 0.0564i
(33,1)	0.0032 - 0.0498i
(34,1)	0.0041 - 0.0322i
(35,1)	0.0020 - 0.0526i
(36,1)	0.0026 - 0.0381i
(37,1)	0.0042 - 0.0591i
(38,1)	0.0054 - 0.0388i
(39,1)	0.0016 - 0.0737i